Mathematical Modeling of Influenza Infection in Humans

BY

AKSHAYA SRUTHI TIRUPATHI POLAEPALLI
B. Tech., Anna University, 2012

THESIS
Submitted as a partial fulfillment of the requirements
for the degree of Master of Science in Chemical Engineering
in the Graduate College of the
University of Illinois at Chicago, 2016

Chicago, Illinois

Defense Committee:
Belinda Akpa, Chair and Advisor
Vivek Sharma, Chemical Engineering
Lewis Wedgewood, Chemical Engineering

This thesis is dedicated to my beloved parents.

Thank you for all your support.

ACKNOWLEDGEMENTS

It is a great pleasure express my deep sense of gratitude and thanks to my thesis advisor – Dr. Belinda S. Akpa – for her consistent guidance and assistance. Her keen interest, scholarly advice, and timely support helped me to achieve my research objectives.

I would like to thank Dr. Vivek Sharma for the moral support and motivation he provided me throughout my graduate education. I would also like to thank him for being on my committee.

I would like to thank Dr. Lewis E. Wedgewood for taking interest in my research and for being on my committee. I am also grateful for the guidance he provided during my graduate studies.

I would like to thank Dr. Cynthia Jameson for her valuable inputs and comments she provided me.

Finally, I would like to thank my family for their unconditional love and encouragement.

ASTP

TABLE OF CONTENTS

LIST OF TABLES

LIST OF FIGURES

LIST OF FIGURES (continued)

FIGURE PAGE

LIST OF FIGURES (continued)

LIST OF ABBREVIATIONS

HIV	Human Immunodeficiency Virus
WHO	World Health Organization
LRI	Lower Respiratory Infection
CDC	Centers for Disease Control and Prevention
MMWR	Morbidity and Mortality Weekly Report
ODE	Ordinary differential equation
IFN	Interferon
NK	Natural Killer
HCV	Hepatitis C Virus
HBV	Hepatitis B Virus
IAV	Influenza A Virus
SD	System Dynamics
S	Susceptible cells
I	Infected cells
I_1	Latently infected cells
I_2	Actively infected cells
V	Free virions

SUMMARY

The annual epidemic caused by the influenza virus results in approximately 300,000-500,000 deaths worldwide. Also, nearly 3 to 5 million severe cases of influenza are reported across the world every year. Vaccines are the most effective way to control the severity and spread of viral infections. However, there are a number of factors that limit the efficacy of influenza vaccines. Tools that facilitate an understanding of dynamic host-pathogen interactions support the design and optimization of interventions to prevent and treat viral diseases. One excellent tool for characterizing interdependent dynamic phenomena such as host immune responses and viral infection and replication is mathematical modeling.

The main aim of this work was to explicitly model natural killer cell response during influenza infection in humans with a minimum set of parameters. We estimated a physiologically valid range for a parameter governing the activity of natural killer cells with regard to lysis of infected cells. Natural killer cell activity that yielded the expected timing of maximum viral load and maximum natural killer cell population was not sufficient to resolve typical influenza infection during the expected 6-8 day timeframe. Hence, we included a simple antibody-based adaptive immune response to mediate viral clearance. A reasonable range of values for the antibody activation parameter was estimated subject to the constraint of three desired model outcomes: time to maximum viral load, virion clearance time, and time to maximum natural killer cell activity.

1. INTRODUCTION

1.1. Overview of Viral Diseases

Viruses are pathogens that cannot reproduce independently but replicate within the cells of another organism (i.e. the host). Viruses hijack the cellular machinery of host cells to replicate the viral genome. The new viral material is packaged into particles (virions) that are released by the infected cell which can then infect other cells. In addition to the infectious agent being passed between individual cells of the host, viral infections are contagious and can be transmitted from one host to another. Possible routes of virus transmission include air-borne, water-borne, and direct contact with various body fluids.

Viral infections can create a significant disease burden, with rapidly transmitted lethal strains having the potential to wipe out large populations – particularly prior to the advent of vaccines. For example, smallpox was a highly contagious viral disease that caused about 100 million to 300 million deaths in the 20th century.[1] In 1918, the Russian Flu infected over 500 million people worldwide, with a fatality rate of 10-20%.[2] Influenza, human immunodeficiency virus (HIV), hepatitis B/C, and measles are all viral diseases that have caused high mortality rates in the 21st century.[3-7] With the human population expanding geographically into areas that bring people into closer contact with wildlife, and the pace of world travel significantly increasing the geographic scope of transmission, the potential for rapid spreading of emerging viral diseases such as Ebola[8] or Zika[9] is of significant concern. In short, viral diseases pose a persistent and global threat to public health.

1.2. Mortality in Humans due to Influenza Infection

Lower respiratory infections in particular pose a serious health concern, causing a greater number of diseases and deaths than viruses more commonly thought of as severe, such as HIV. In Figure 1, data is compared between lower respiratory infections (LRIs) and HIV in the year 2013.[10-12] This data clearly indicates that both the number of people infected and those who died from LRIs in 2013 far outnumbered those with HIV infections. According to the data published by World Health Organization (WHO), lower respiratory infections were the third leading cause of mortality in 2015 (3.2 million deaths), surpassed only by ischaemic heart disease (7.6 million deaths) and stroke (6.7 million deaths).[13]

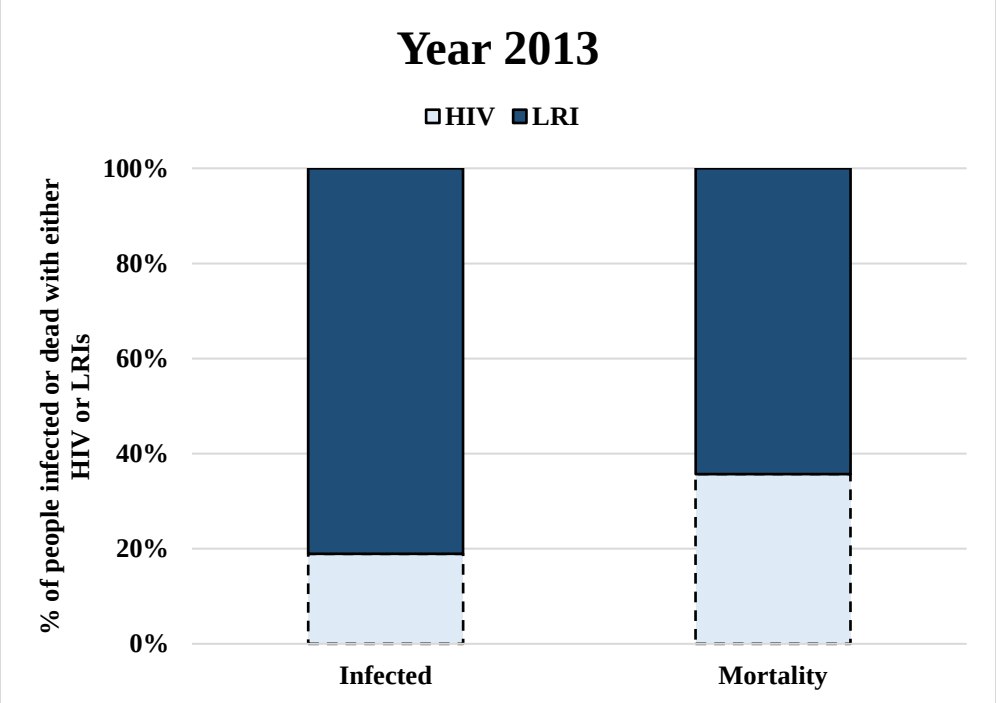

Figure 1. Infection and mortality rates of HIV and LRIs worldwide in 2013.

Epidemics of respiratory diseases occur frequently and with seasonal regularity. Figure 2 depicts the fraction of deaths across 122 cities in the United States that could be attributed to pneumonia and influenza between 2013 and early 2016.[14] Each time the red frequency curve exceeds the region defined by black line (the epidemic threshold), the infectious disease has spread across a large enough population to be described as an epidemic. The epidemic threshold is exceeded shortly before the 10th week of each year despite preventive and clinical measures taken to control the seasonal outbreak of infection (such as flu vaccines).

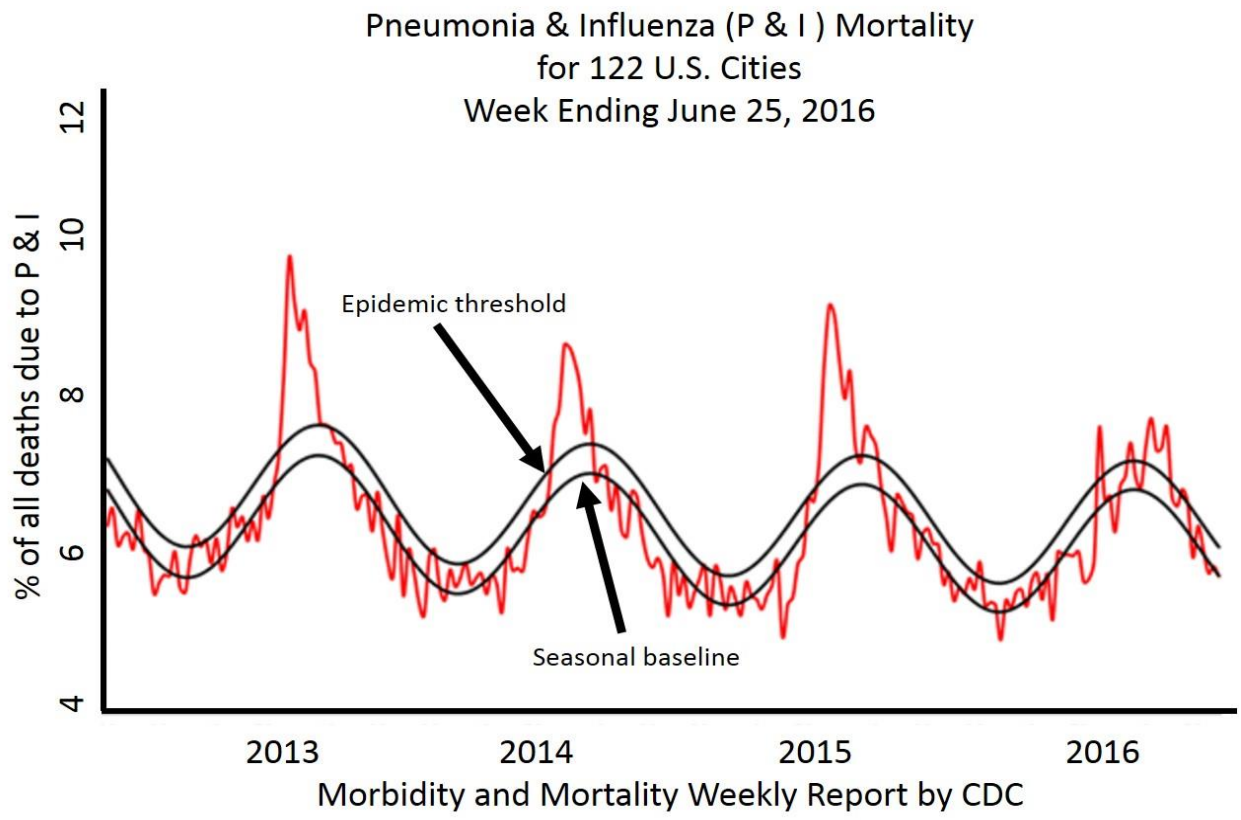

Figure 2. Morbidity and Mortality Weekly Report (MMWR) showing the percentage mortality in 122 U.S. cities due to pneumonia and influenza infections.

The term pandemic is used to describe the spread of an infectious disease across more than one continent. The influenza virus has been responsible for several pandemics, including at least four in the 19th century and three outbreaks in the 20th century.[15] The 1889-1890 flu pandemic affected roughly one-third of the world's population[2], while the first H1N1 influenza pandemic of the 20th century (the so-called Spanish Flu) killed at least 40 million people.[16-18] The first pandemic flu of the 21st century is estimated to have caused 284,500 deaths in 2009.[19]

1.3. Challenges in Controlling Influenza Infection

Vaccines provide immunity against viral infections by preparing the host to identify and eliminate a particular virus. They are the most effective way to control the severity and spread of viral infections. Several viral diseases, including small pox have been entirely or nearly entirely eradicated by vaccination.[20] Unfortunately, vaccines are not effective in controlling influenza infection. Every year vaccines are distributed to control the seasonal outbreak of influenza infection. However, influenza has not been eradicated. In fact, the vaccines circulated during last flu season were only 60% effective.[21, 22]

There are a number of factors that limit the efficacy of influenza vaccines. For one, influenza occurs as multiple viral strains, and the virus undergoes rapid mutation (changes in the genetic make-up) yielding ever new viral variants. Seasonal influenza vaccines are designed to target only the most prominent viral strains. Rapid mutation increases the likelihood that vaccine-resistant strains later emerge. Likewise, mutation increases the chance of the virus becoming resistant to antiviral drugs. Neuraminidase inhibitors, the drugs typically used to treat influenza

infections in the United States, target and thereby inhibit a specific viral protein. A single-residue genetic mutation can alter the nature of this protein sufficiently to render these drugs ineffective.[23,24] Difficulties in controlling influenza result in approximately 300,000-500,000 deaths globally each year.[25]

1.4. Characteristics of Primary Influenza Infection

Both vaccines and antiviral drugs represent attempts to modulate the host-pathogen interaction in a way that gives the host's immune system a better chance to resist and control infection. The influenza virus initially infects lung epithelial cells. These cells produce further viral particles, but also release chemical signals (i.e., cytokines) that are part of the body's first line of defense, the so-called innate or non-specific immune response. The release of cytokines activates a cascade of events whose objective is to (i) protect as-yet uninfected cells, (ii) eliminate infected cells, and (iii) clear free virus particles. What follows is a highly simplified overview of the nature of the events that make up an immune response to viral infections.

A key signaling protein involved in limiting the progress of infection across a population of cells is interferon type 1 (IFN-1). Interferon, when released by infected cells or phagocytic virus-clearing cells, alerts other cells to the presence of a pathogen. Cells that are susceptible to infection respond by adopting a resistant (anti-viral) state, expressing genes that will limit the ability of a virus to replicate successfully. [26] Interferon also activates cells of the immune system that are capable of lysing infected cells – thereby eliminating cells that are churning out additional virions. While cell-lysing immune cells come in a number of types, those that are activated by

interferon in the earliest stage of infection are called Natural Killer (NK) cells.[27-29] The NK cells in turn produce a form of interferon signaling protein (IFN-γ) that activates other cells of the immune system that contribute to a pathogen-specific defense strategy.

It is this pathogen-specific immunity (adaptive immunity) that is responsible for the efficacy of vaccines. Having encountered a new pathogen, the immune system learns to recognize the particular virus and targets it for clearance both directly (by removal of virus particles) and indirectly (by augmented lysis of infected cells). Adaptive immunity involves (i) presentation of virus antigens to lymph nodes and other sites of immune cell storage to inform lymphocytes as to the nature of the specific pathogen[30], (ii) expansion of cytotoxic T lymphocytes (T-cells), immune cells equipped with specific receptors required to recognize and kill infected cells[31,32], and (iii) expansion of B-cells, immune cells that produce antibodies to bind and inactivate viral particles[33,34]. These cellular immune effectors are accompanied by soluble effectors in the form of additional signaling chemicals that help to orchestrate the regulated growth of lymphocyte population and their targeting to sites of infection. Memory T-cells linger within the body after the infection has been cleared, preserving that pathogen-specific immune function so that it can be rapidly implemented upon future challenge by the same virus.

1.5. Mathematical Models as a Tool to Interrogate Influenza Infection

Tools that facilitate an understanding of the dynamic host-pathogen interactions support the design and optimization of interventions to prevent and treat viral diseases. One excellent tool for characterizing interdependent dynamic phenomena such as host immune responses and viral

infection and replication is mathematical modeling. Ideally, systems models of immune dynamics capture our best current understanding of the factors that contribute to success or failure in controlling the evolutions of viral load and allow for hypothesis testing and hypothesis formulation with regard to the value of intervention strategies – particularly as said strategies depend on the varying infectivity and virulence of the viral pathogen. Thus, mathematical models can be an important part of the toolkit for reducing the global burden of viral disease. Within-host viral kinetic models have been used to characterize the emergence of drug resistance and inter-individual or viral strain-specific variability in infection duration and severity. Such models have also been used to analyze different aspects of immune responses and to evaluate treatment strategies in various viral diseases (e.g. HIV, hepatitis C virus, hepatitis B virus, measles[35-48]).

The mathematical models used to study viral kinetics employ coupled differential equations whose state variables describe populations of key players in the process of infection and immune response (e.g. cells, virions, antibodies). The outcomes of these models are time courses revealing the dynamics of each population [Figure 3]. Model parameters may be adjusted to yield physiologically valid outcomes, as determined by experimental observations.

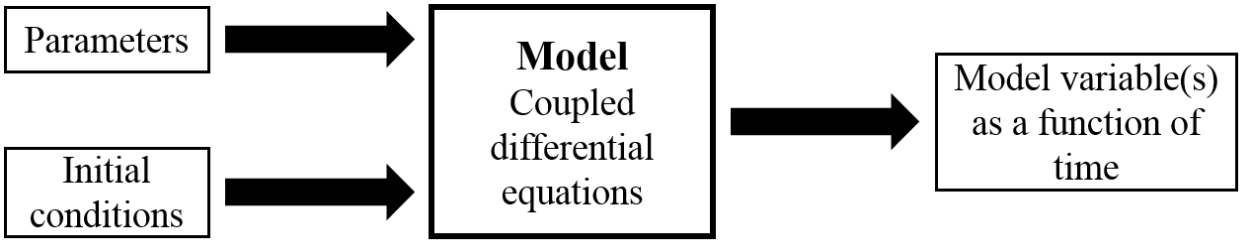

Figure 3. Schematic representation of viral kinetic models.

At minimum, a dynamic model of viral infection should include cells that can be infected, free virions that may infect cells, viral replication by infected cells, and viral clearance from the organism in question. In the case of influenza, lung epithelial cells are the primary population susceptible to infection. Two major approaches are followed with regard to this cell population: models that allow for replenishment of these target cells and those that do not. The latter group of models is most common and is referred to as target cell-limited. They are so called because the progress of infection is limited only by the number of virus-susceptible cells available. Once all cells are infected, the infection must burn itself out over time due to the natural death of infected cells. If a sufficiently robust immune response is represented, then progress of the infection may be halted before complete depletion of the susceptible cell population. Increasingly complex variations on this basic motif have been implemented to consider the role of host immune response and antiviral interventions in determining viral dynamics. A brief summary of models follows.

The first mathematical model of influenza infection was designed by Larson et al.[49] in 1976. This simple model did not make any attempt to explicitly represent the various effectors (cellular or soluble) of the immune system, but rather connected four non-specific compartments to a virus accumulator compartment whose dynamics were fit to data obtained for H3N2 influenza viral load in mice. Fits were reasonable, yielding different parameter values for each of the 3 tissues considered. Eighteen years after that initial attempt, a second mathematical model of influenza infection was reported by Bocharov and Romanyukha.[50] While Larson et al. endeavored to create the simplest possible model that would capture observed viral dynamics, Bocharov and Romanyukha developed a model whose structure is grounded in the known biology and physiology

of host-pathogen interactions and the extant body of knowledge regarding the time course of 'normal' influenza infection. To date, this model of influenza A virus in humans is the most complex and comprehensive published example. It contains 60 parameters and attempts to build a very detailed description of important components of both the innate and adaptive immune responses. Ten state variables encompass the time-dependent viral load, virus-susceptible cells, virus-clearing phagocytic cells, activated B and T lymphocytes, and virus-neutralizing antibodies.

Twelve years later, the pendulum swing was back in the direction of simplicity, with the 2006 model of Baccam et al.[51] Here a minimal model shaped around key biological processes was used to interrogate the relevance of a delay between cell infection and cell productivity vis-à-vis releasing new viral particles. Human influenza A virus (IAV) infection with and without an eclipse phase of infection (time lag between virus entry into a cell to new virus production by the cell) were modeled.[51] A target-cell-limited model was employed and host immunity was represented by an interferon mediated inhibition of virion production by infected cells. This inhibition was considered either to slow the transition of cells from the eclipse phase to the virion producing phase or to slow the rate of production of virions by productively infected cells. Inclusion of the interferon effect allowed for bimodal concentration-time curves for viral load, an outcome occasionally observed in experimental studies. This modeling effort also applied the viral kinetic approach to predicting the efficacy of antivirals.

Likewise, Handel et al.[52] extended the target-cell-limited model approach to examine the effectiveness of neuraminidase inhibitors during IAV infection in humans. Neuraminidase

inhibitors are anti-viral drugs that suppress the action of an enzyme (neuraminidase) essential for viral reproduction. For the purposes of examining how viral resistance to drugs evolves and the possibility of transfer of resistance to another host, Handel et al. chose to represent two different virus populations in their model: one sensitive to antiviral drug and one resistant to it. Host immunity was represented as an exponentially growing immune response capable of augmenting viral clearance (i.e. an antibody-like response). The host-to-host spread of the drug resistant strain was found to depend on the robustness of individual host immune responses, timing of drug treatment (earlier is better), and efficacy of the drug. Despite several limitations, such as the large uncertainty in parameter estimates made based upon scarce data, the approach demonstrates that simple within-host target-cell-limited models can be valuable in predicting the efficacy of antiviral therapies vis-à-vis the spread of infection across a population.

Dobrovolny et al.[53] also attempted to analyze the efficacy of neuraminidase inhibitor, but chose to consider not multiple viral strains, but rather multiple cell populations of differing susceptibility to infection and differing rates of virion production. Their aim was to consider whether neuraminidase inhibitors would have utility in human infections with avian influenza, and whether there is value to treatment with these antivirals at more than 48 hours post infection. The two-cell model was proposed as a possible explanation for the prolonged high levels of virus observed in patients infected with avian influenza. This approach successfully reproduced the prolonged viral loads which is a characteristic of avian influenza and suggested that, while not of value in the case of human IAV, late intervention with antiviral drugs should impact health outcomes in the case of avian influenza – a promising conclusion for the case of a viral disease

where patients frequently do not receive prompt medical intervention. Notably absent from the Dobrovolny model is any explicit immune response. While reasonable fits to clinical data were obtained in most cases, in the cases of two patients, a rebound of virus levels was predicted to follow cessation of drug treatment. This rebound was not observed in the clinical data, and is likely a direct consequence of the model failing to capture the multifaceted nature of host immune response.

Hancioglu et al.[54] likewise observed rebound of virus in their models of human IAV infection. While the model included mechanisms of both innate and adaptive immunity in the form of interferon-induced protection of susceptible cells and antibody-mediated viral clearance, it also explicitly incorporated an evolution of antigenic specificity. That is, the model discriminates between existing antibodies that may have limited compatibility to the virus and strain-specific neutralizing antibodies. Hence, the model explicitly accounts for time taken for the humoral component of immune response to give rise to antibodies specific to viral strain in question. The resulting 10 differential equations and 27 parameters yielded a dynamic system whose outcome would be asymptomatic disease, typical disease, or severe disease depending on the initial quantity of virus. Furthermore, these authors demonstrated the relevance of a robust adaptive immune response that yields both high levels of antibodies and rapid development of antibody specificity, the absence of which led to a chronic reservoir of virus. The requirement for robust adaptive immunity in valid mathematical models of influenza infection has also been reported for mice.[55]

Recently, mathematical modeling efforts for influenza viral infection have turned toward the question of secondary bacterial infections. Researchers have examined how bacterial infections can drive rebounds of influenza viral loads in mice.[56] Others have addressed the question of whether antiviral treatments help control secondary bacterial infections in mice.[57] Still others have considered viral co-infection, choosing to design mathematical models that capture the competing dynamics of multiple influenza strains of varying pathogenicity[58] or the potential for influenza virus to infect cells other than lung epithelial cells.[59]

Though the state-of-the-art modeling of influenza infection is moving towards the modeling of secondary bacterial infections and different pathogenic strains of virus, fundamental questions remain as to the quantitative modeling of typical influenza infection. For example, there is evidence in the literature that natural killer cells play a crucial role in controlling the initial rise of influenza infection. Natural killer cells begin their activity within a few hours post infection and help in controlling the infection by lysing infected cells.[60-64] Natural killer cells also secrete cytokines that aid in the activation of adaptive immune response.[65-70] Furthermore, experimental studies show that the effectiveness of natural killer cell activity is a critical determinant of the severity of influenza infection. A strain of influenza that can evade the natural killer cell response, will result in the host experiencing chronic and prolonged infection.[71-73] Although natural killer cells have been known to play a vital role in controlling influenza infection, none of the models discussed above attempt to explicitly capture this biological response. A first attempt to model natural killer cell activity in human IAV infection was demonstrated by Canini and Carrat (2011).[74] A target-cell-limited model was used in combination with a symptom dynamics modeling

approach to examine the evolution of infection and its interplay with an index of symptom severity. Natural killer cell activity was assumed to increase at a rate proportional to levels of immune signaling proteins (lumped cytokines). Cytokine levels were, in turn, said to grow with a rate dictated by the population of infected cells. Model parameters were estimated by fits to both experimentally determined viral loads and symptom severity scores, but no experimental measures of cytokine or natural killer cell levels were employed. Furthermore, there was no adaptive component in this model, so the interplay between adaptive (late-acting) and innate (early acting) immunity was not examined.

In this thesis, we identify a physiologically plausible range of natural killer cell activity against infected cells using viral kinetic modeling. The model parameter values are chosen to give outcomes that compare favorably with what is known about the normal course of human influenza infections. To the best of our knowledge, this is the first attempt to explicitly model natural killer cell populations in influenza dynamic models. We do so without invoking interferon or other cytokines as a mediator of natural killer cell activity, thereby limiting the total number of model parameters. In addition, we consider the necessity of accounting for natural death of cells that are in a non-productive infected state. We then explore antibody activation as a minimal representation of the adaptive immune response, showing that this means of neutralizing free virus particles is necessary to ensure resolution of infection within a physiologically reasonable time frame, but has little impact on the initial severity of infection. Thus, adaptive immunity may indeed need to be considered in any model that attempts to describe more than the first ~3 days of infection. We also demonstrate the complementary nature of the innate and adaptive immune

responses and highlight the difficulty this complementarity presents in the context of parameter estimation from one-dimensional data sets (e.g. from measures of viral load only).

1.6. Objectives and Goals of Current Study

First, a simple target-cell-limited model (reference model) without any explicit immune response was developed. Next, we considered the relevance of accounting for natural cell death amongst cells in a latent phase of infection. Death of this cell population is typically neglected in viral kinetic models, while natural death of virion-producing infected cells is explicitly considered.[51,53,74] Chen et al.[75] do include a natural death term for infected cells in the latent phase. No justification is provided for either approach. With simple models being more amenable to both parameter estimation and scaling analyses, but more complex models allowing for more complete interrogation of biological mechanisms, it is important to assess the validity of including or excluding such a term. We attempted to clarify the impact of this term on influenza dynamics by performing a comparative study of the two approaches.

Finally, we developed a simple natural killer cell response model in which natural killer cell activation was assumed to be proportional to the population of infected cells. The effectiveness of natural killer cells with regard to elimination of infected cells was captured by a destruction parameter (rate constant). We determined upper and lower limits on the activity of natural killer cells by considering the ability of this single immunity effector to resolve viral load in a physiologically relevant time frame. Hence, we determine a physiologically plausible range of values for the destruction parameter. Within this range of activity, model predictions indicated that

natural killer cells should be successful in controlling influenza during the initial stage of infection. However, the action of natural killer cells alone was not sufficient to completely resolve the infection. A simple antibody response was introduced to explore the role of adaptive immunity in resolving the infection. The physiologically valid range of natural killer cell action on virus-infected cells was reconsidered in the context of this adaptive response, and the upper and lower limits of antibody activation were also examined.

2. REFERENCE MODEL (MODEL 1)

2.1. Introduction

We begin by establishing a reference model that represents the minimum features of infection. The model includes three variables, namely susceptible cells (S), free virus particles (virions, V), and infected cells (I) [Figure 4]. The model is target-cell-limited and similar to that reported by Baccam et al.[51] for influenza infection in humans.

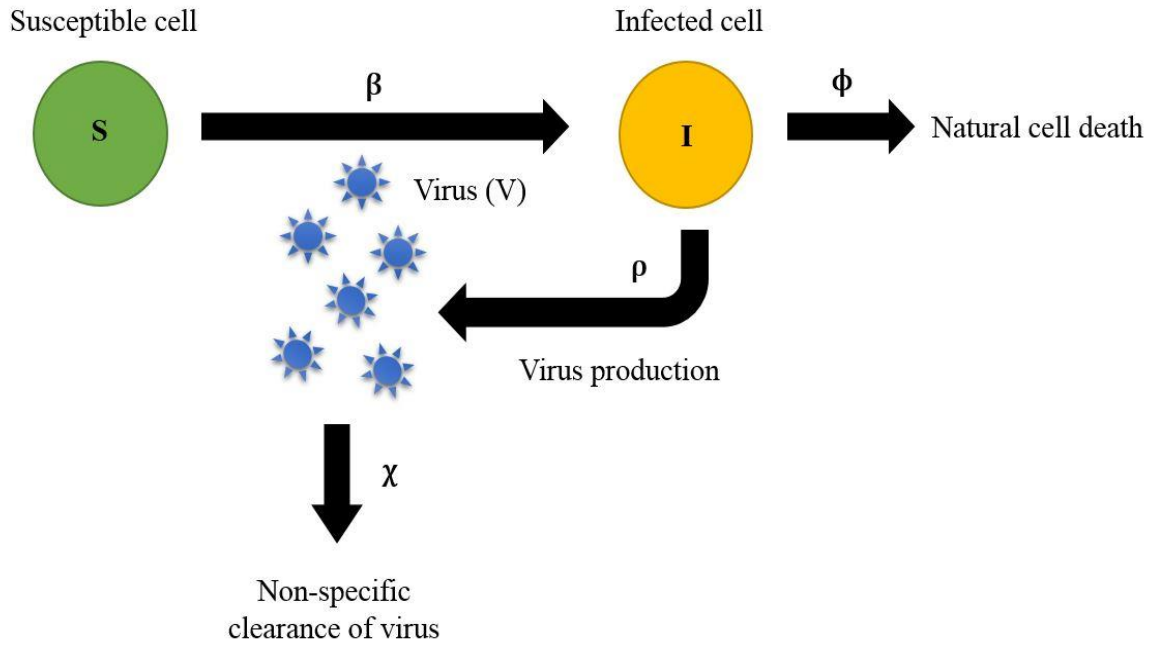

Figure 4. Schematic representation of in Model 1. β, ρ, ϕ, and χ are rate constants governing mass action and exponential decay terms describing system fluxes. S – susceptible cells; I – infected cells; V – free virus particles.

The following assumptions are made in constructing this reference model.

i. All susceptible cells are capable of becoming infected.

ii. Infection requires one free virus particle to enter a susceptible cell. The rate constant for infection is represented by the parameter β virion^{-1} day^{-1}, and the rate of infection can be described using mass action kinetics considering the populations of susceptible cells and free virions.

iii. Once infected, cells release new infectious virus particles at a rate of ρ virions per cell per day.

iv. The number of free virions depleted during the process of cell infection is assumed to be negligible[51].

v. Infected cells have a finite natural lifetime and their death is described as an exponential decay with rate constant ϕ day^{-1}.

vi. Regeneration of susceptible cells can be neglected in the early stages of influenza infection, as the depletion of cells due to infection occurs at a rate 100 times greater than cell production ($\lambda = 6.25\times10^{7}$ day^{-1}).[76] Baccam et al.[51] included a regeneration term for susceptible cells and found that it did not result in a better fit to the experimental data. Similarly, the depletion rate of susceptible cells due to infection was found to be 10 times greater than the natural cell death rate of susceptible cells ($\varphi = 0.0625$ day^{-1}).[76] We choose here to neglect the death rate of susceptible cells.

vii. No explicit immune response factors are considered, but free virions are cleared from the host via a non-specific first order mechanism with decay rate constant χ day^{-1}.[51]

Based on these assumptions, the governing system of ordinary differential equations (ODEs) is as given in Equations 1-3. These equations were solved using the Simbiology toolbox in MATLAB 8.5 (R2015a) with ODE solver *ode15s*, which is an implicit multistep method.

$$\frac{dS}{dt} = -\beta[S][V] \quad [1]$$

$$\frac{dI}{dt} = \beta[S][V] - \phi[I] \quad [2]$$

$$\frac{dV}{dt} = \rho[I] - \chi[V] \quad [3]$$

The model parameters were taken from Chang and Young[76]. The values correspond to physiologically reasonable ranges originally estimated by Bocharov and Romanyukha[50], who fitted their model to experimental data (viral load, immune cells and antibodies). Indeed much of the prior work on modeling influenza in humans has been parameterized based on the pioneering efforts of Bocharov and Romanyukha.[50,54,75,76] The initial conditions and model parameters are outlined in TABLE I, and TABLE II, respectively. We initiate the model with 10^9 susceptible (healthy) cells, which corresponds to the steady-state level of cells in a healthy adult.

TABLE I. Initial conditions for the differential equations discussed under reference model.

Initial Conditions	**Value**	**Units**	**Reference**
Susceptible cells (S_0)	10^9	cells	76
Infected cells (I_0)	0	cells	76
Virus (V_0)	10^7	virions	76

TABLE II. Parameters values for the differential equations discussed under reference model.

Model Parameters	**Value**	**Units**	**Reference**
Infection rate (β)	10^{-10}	virion^{-1} day^{-1}	76
Natural death of infected cells (ϕ)	1	day^{-1}	76
Production of virus (ρ)	340	cell^{-1} day^{-1}	76
Non-specific clearance of virus (χ)	2	day^{-1}	76

2.2. Results and Discussion

Time courses for the model variables S, I, and V are shown in Figure 5 and Figure 6. The population of susceptible cells undergoes rapid decline during the first few days of infection. Within 3 days post infection, more than 90% of susceptible cells were infected, giving rise to a maximum in the number of infected cells at 2.44 days post infection [Figure 5]. The maximum number of infected cells occurs when the rate of infection is equal to the rate of natural cell death of infected cells, giving the following relationship for the maximum population of infected cells.

$$I_{max} = \frac{\beta}{\phi}([S][V])|_{t(I_{max})} \quad [4]$$

This maximum is dictated by the relative values of rate constants β and ϕ. If ϕ is dictated mainly by cell type and β is dictated by infectivity of the virus in question (i.e., ability to efficiently enter cells it encounter), then the number of cells infected is primarily determined by the viral strain in question.

While the population of infected cells peaks at 2.44 days, the viral load (population of free virus particles) continues to increase. This is because each infected cell is capable of producing more than one progeny virion. The average rate of influenza virus production per infected cell (n) can be defined as the product of rate constant for virus production and life-time of an infected cell.

$$n = \rho * \left(\frac{1}{\phi}\right) = 340 \quad [5]$$

Hence, for a peak population of 5.9×10^{8} infected cells, one can expect ~ 10^{11} free virions to be produced over the course of the infection. Indeed, the peak population of free virions is 7.68×10^{10}, achieved at 2.87 days post infection [Figure 6]. The maximum in the viral load lags behind the maximum in the infected cells by 10 hours.

After 2.44 days, despite continued growth in the population of free virions, the population of infected cells declines because the population of cells available for infection is substantially depleted.

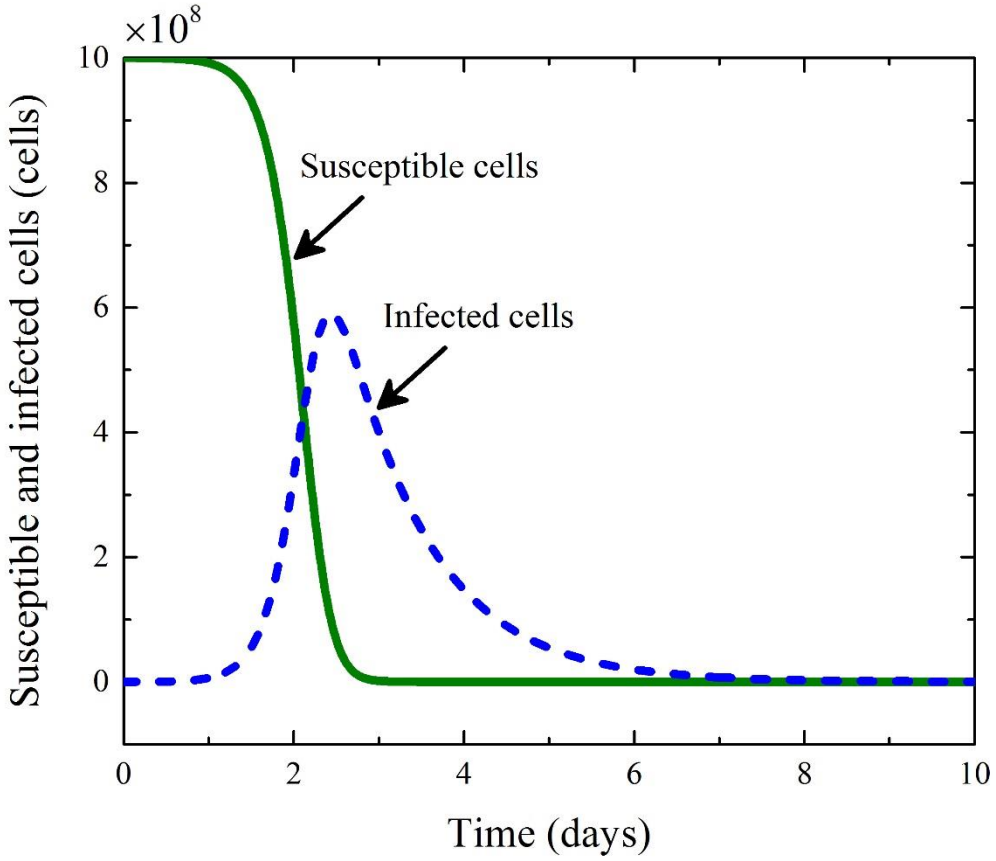

Figure 5. Reference model: Time dependence of susceptible cell (solid green line) and infected cell (dashed blue line) populations over ten days post infection.

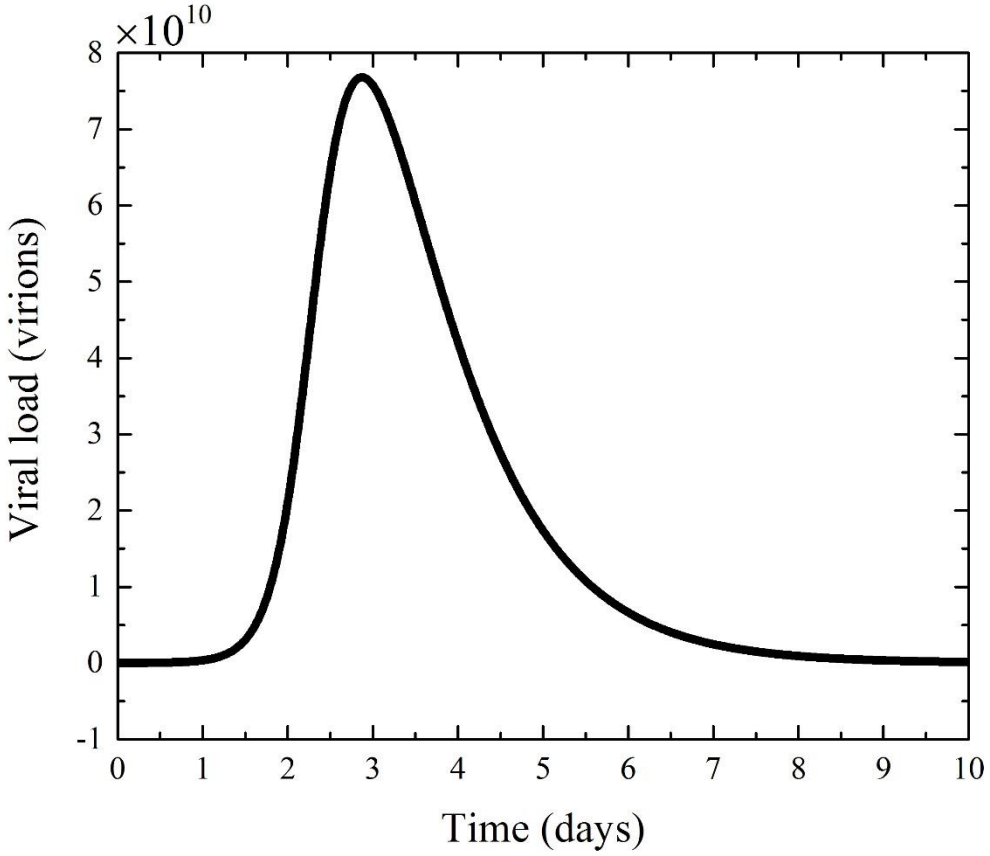

Figure 6. Reference model: Evolution of viral load over ten days post infection.

2.3. Summary

The reference model demonstrates the minimal features of an IAV infection in humans. Model dynamics for the 3 state variables were briefly discussed. The model is target-cell-limited, so infection should only cease upon exhaustion of the susceptible cells. Virus production ceases only when all infected cells are depleted. In the 10 day timeframe considered, more than 95% of healthy susceptible cells were depleted, and the viral load remained non-zero at the 6-8 day time point when typical influenza infections is known to be resolved. This prolonged presence of the

virus reservoir and exhaustion of susceptible cells is to be expected, as there are no mechanisms of immune response captured in the model. Therefore, the next step is to include specific immune response factors in the model and interrogate the effect of both innate and adaptive immune responses on the viral load (Chapter 4). In the following chapter, we discuss a comparative study on the role of natural cell death in the context of a time lag occurring between initial infection of a cell and that cell becoming capable of producing new virus particles – i.e. a latent phase of infection.

3. LATENT PHASE MODEL (MODEL 2)

3.1. Introduction

Experiments have shown that there may be a time lag of as much as 6-12 hours between the time that a cell is infected by the influenza virus and the time at which that cell displays neuraminidase enzymatic activity, a marker of virus reproduction.[77] This biological delay in the virus production can be captured in a viral kinetic model by proposing two different population of infected cells: one that has been penetrated by a viral particle but has not yet synthesized and repackaged viral protein for excretion as a new free virion; and one that is actively secreting free virions. We refer to these to populations as latent and active, and denote them with state variable I_1 and I_2, respectively [Figure 7]. The existence of a latent phase of infection has been considered in modeling approaches adopted by other researchers, but the relevance of including[75] or disregarding death of latently infected cells has not been justified.[51,53,74] The main objective of this chapter is to analyze the quantitative and qualitative differences (if any) in the model outcome when we include [Equation 7] or neglect [Equation 8] the possibility of natural cell death for cells in the latent phase of infection.

The primary assumptions stated under the reference model 1 are assumed to be true for latent phase models, with minor changes in the model equations as formulated as below.

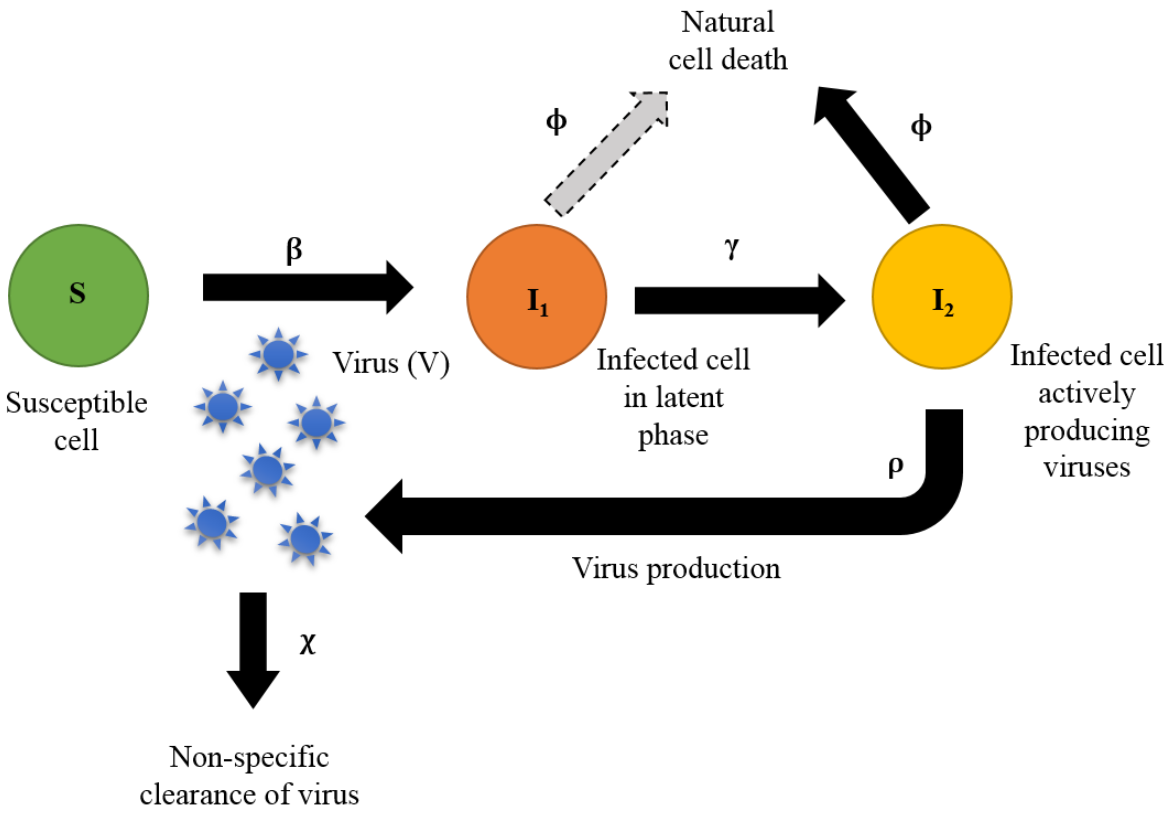

Figure 7. Schematic representations of equations discussed under latent phase model. The dashed arrow indicates that in case (a) the natural death of latently infected cells is included, but in case (b) it is assumed to be negligible.

$$\frac{dS}{dt} = -\beta[S][V] \quad [6]$$

$$\text{Case (a): } \frac{dI_1}{dt} = \beta[S][V] - \gamma[I_1] - \phi[I_1] \quad [7]$$

$$\text{Case (b): } \frac{dI_1}{dt} = \beta[S][V] - \gamma[I_1] \quad [8]$$

$$\frac{dI_2}{dt} = \gamma[I_1] - \phi[I_2] \quad [9]$$

$$\frac{dV}{dt} = \rho[I_2] - \chi[V] \quad [10]$$

The equation for susceptible cells [Equation 6], initial conditions, and parameter values are the same as in the reference model [TABLE I and TABLE II]. We assume that cells in the latent phase of infection (I_1 cells) will start producing virions after 6 hours following virus entry into the cell. Hence I_1 cells become actively infected cells with a rate constant of $\gamma = 4\ day^{-1}$ [77] [Figure 7]. As in the reference model, parameter ϕ governs the rate of natural cell death of infected cells (same for both I_1 and I_2), and χ governs viral clearance. The rate of virus production is assumed to be directly proportional to the number of actively infected cells (I_2 cells) [Equation 10].

3.2. Results and Discussion

Time courses for the four state variables are shown in Figures 8-10. Assuming that the natural death term (ϕI_1) to be negligible did not bring about any qualitative changes in the susceptible cell population. There is a rapid decline in the number of susceptible cells during the initial phase, and more than 95% of the cells were depleted within 10 days post infection in both cases (a) and (b). Within 4 days post infection, more than 90% of the susceptible cells were infected in both cases. However, neglecting the natural death of latently infected (I_1) cells produced a slightly earlier decline in the population of susceptible cells [Figure 8].

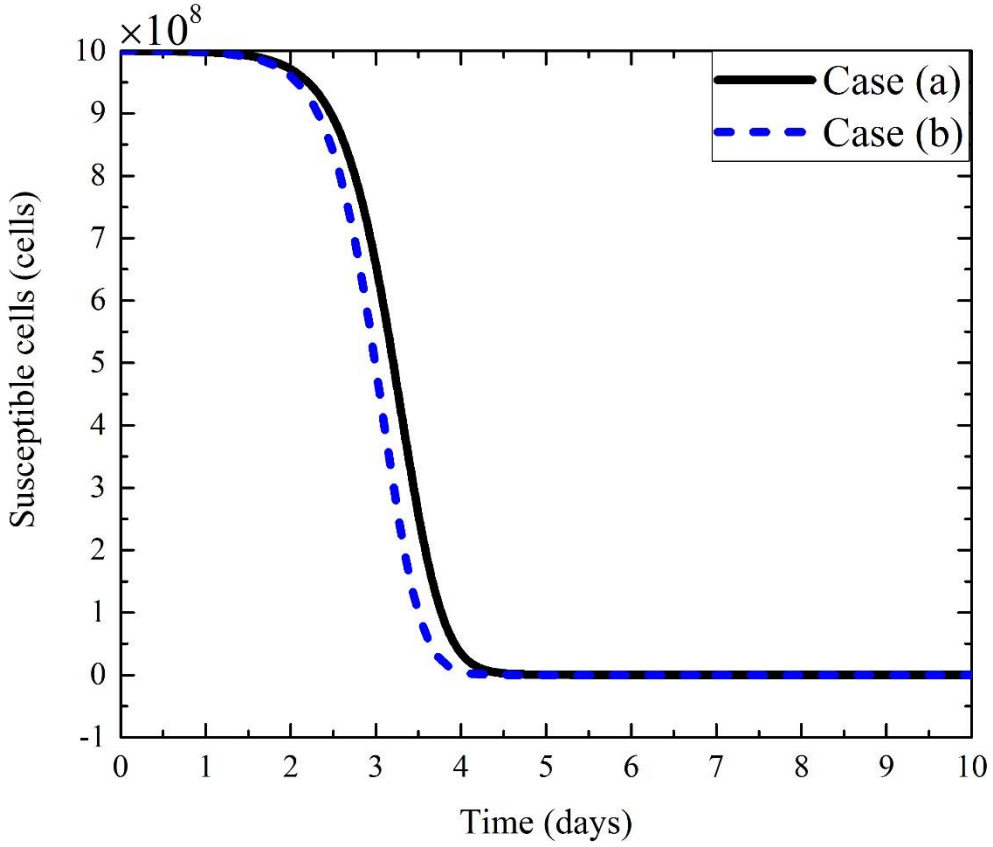

Figure 8. Change in the number of susceptible cells with time in latent phase model: Case (a)-solid black line and Case (b)-dashed blue line.

At the maximum of $I_1(t)$, the relations given in Equations 11 and 12 hold in the case of including and neglecting latent phase cell death, respectively.

$$\text{Case (a): } I_{1,\max} = \left(\frac{\beta}{(\gamma+\phi)}\right)[S][V] \quad [11]$$

$$\text{Case (b): } I_{1,\max} = \left(\frac{\beta}{\gamma}\right)[S][V] \quad [12]$$

From this, it is clear that the effect of the natural death term is to reduce the maximum in the latent cell population. In the absence of latent (I_1) cell death, the maximum number of latently infected cells is 24% greater [Figure 9-solid black line and dotted orange line]. This leads to a corresponding increase in the maximum number of actively infected (I_2) cells – 22% greater in when latent phase cell death is neglected [Figure 9- dashed-dotted blue line and short dashed violet line]. The maximum in the I_2 cell population lags behind the maximum in the I_1 population by 11 hours in both cases (a) and (b). The maximum in the latent phase cell population occurs 6 hours earlier when cell death is neglected. However, both time courses exhibit a single maximum, with a rapidly decreasing cell number thereafter. It is not trivial to state the likely impact of virus infectivity on the latently infected cell population. The latent phase mathematical model includes two parameters that can be interpreted as being associated with viral pathogenicity, β and γ. One governs the efficiency of initial infection, while the other describes how quickly an infected cell begins contributing to the free virion population. Highly infective strains thus may be characterized by an increase in each of these parameters, which appear as a ratio in the expression for peak I_1 cell population. The magnitude of the latently infected population is thus not particularly telling the case of acute infection. What is important for rapid establishment of

infection is a large flux towards the actively infected (I_2) state, which is favored by increasing values of both β and γ.

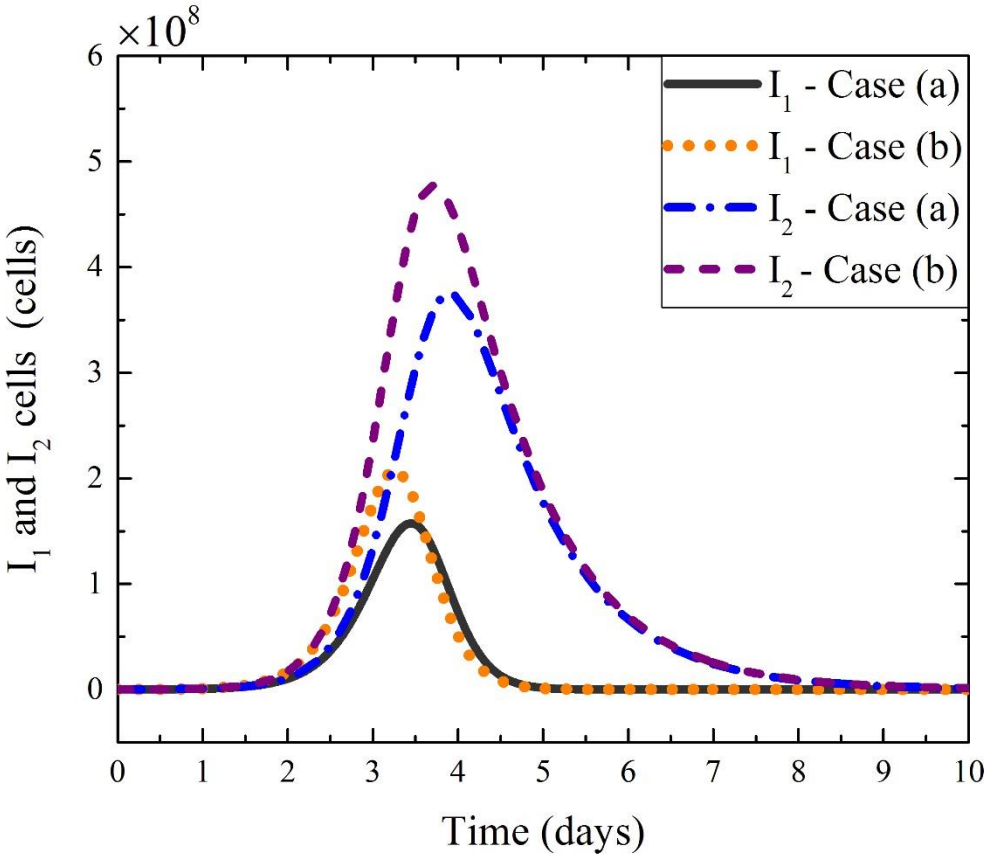

Figure 9. Population of I_1 and I_2 cells for both cases (a) and (b) discussed under latent phase model.

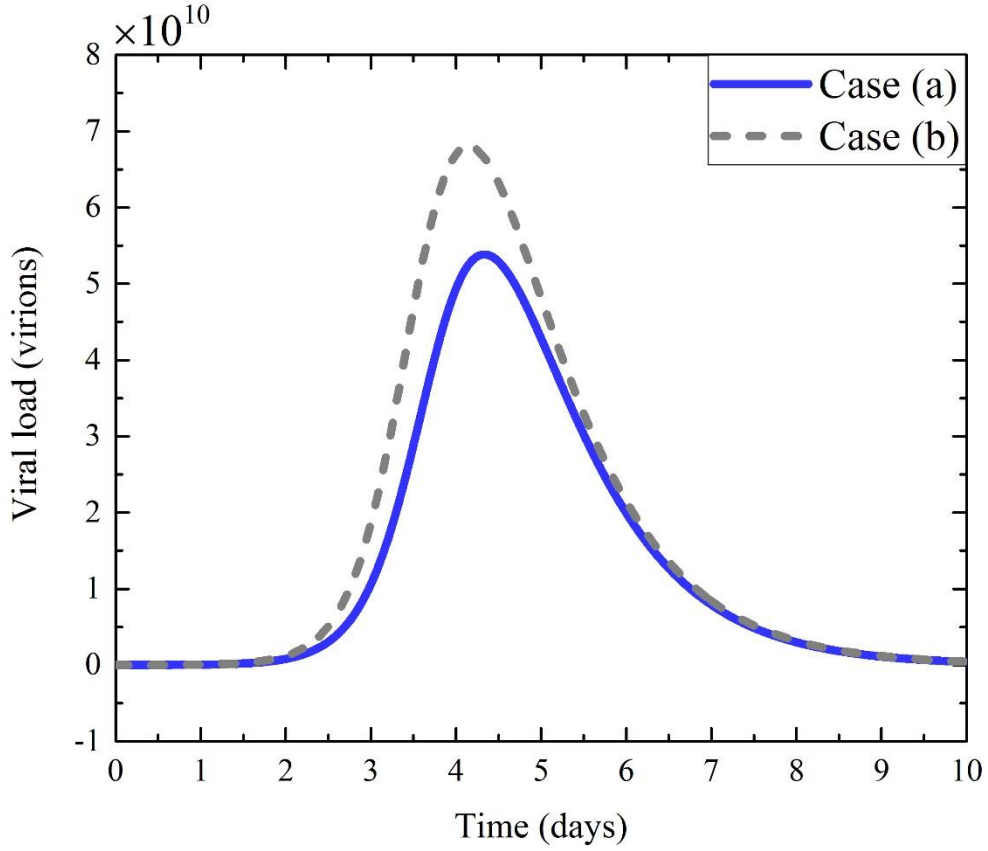

Figure 10. Viral dynamics observed when latent phase cell death is (a) included and (b) neglected.

As the population of infected cells (both I_1 and I_2 cells) was higher in the absence of latent cell death, a higher viral load is expected. The virus maximum was achieved 4.6 hours earlier when cell death was neglected, and the viral load at the maximum was found to be 21% higher [Figure 10].

Finally, the quantitative differences between reference and latent phase models are compared in Figure 11. The virus maximum in the reference model was achieved at 2.87 days post

infection, but in the latent phase model it was achieved at ~4 days post infection. When compared to the reference model, the maximum virion population was 30 % and 11 % lower in the latent phase model for including and neglecting cell death, respectively. This decrease in the magnitude of maximum viral load is a consequence of splitting the infected cell population between latent and active phases [Figures 10 and 11].

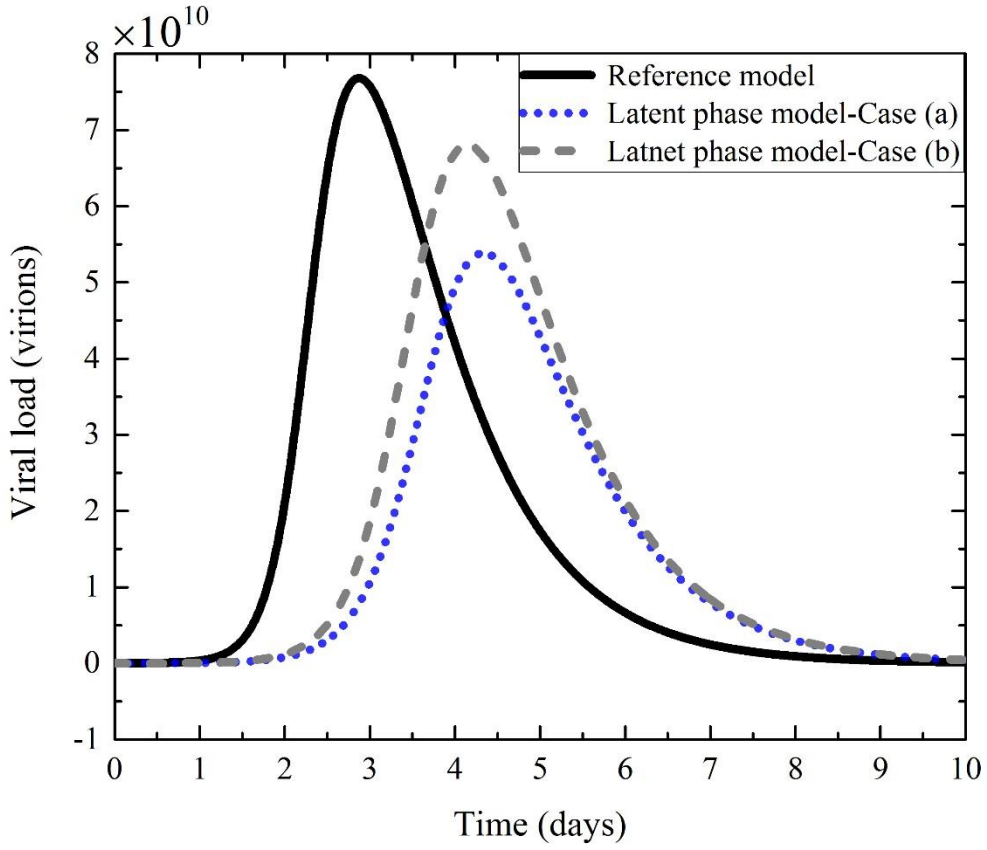

Figure 11. Comparing viral loads between reference model (solid black line) and latent phase model (case (a)-dotted blue line and case (b)-dashed gray line).

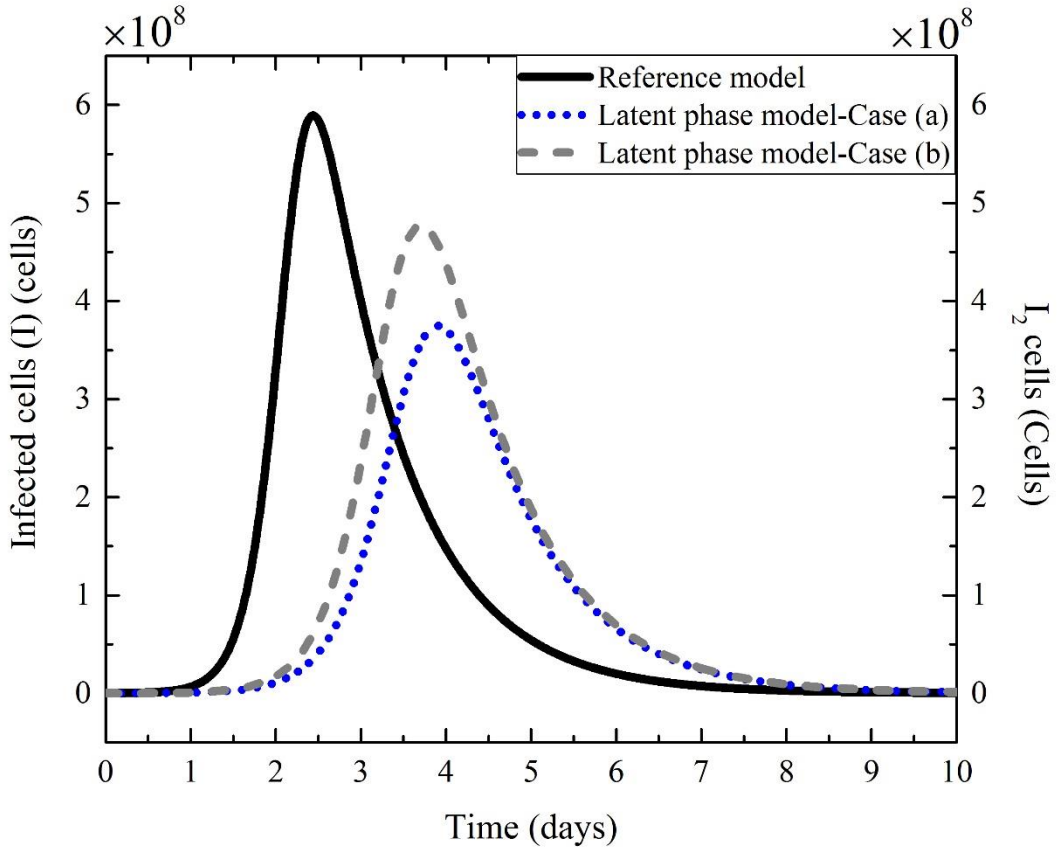

Figure 12. Comparing the number of infected cells (I) in reference model (solid black line) with the actively virus producing infected cells (I_2) in latent phase model (case (a)-dotted blue line and case (b)-dotted gray line).

3.3. Summary and Conclusions

Influenza infection dynamics in latent phase models were compared in this chapter. Two cases, one with and without natural cell death of infected cells in a latent phase, were considered. Significant quantitative differences were observed between the two cases. In particular, neglecting a term for cell death yielded larger numbers of infected cells and a greater viral load. We note that the flux of cells from a latent state to an active state (governed by rate constant $\gamma = 4$ day^{-1}) was 4

times greater than the flux from toward natural death (governed by rate constant $\phi = 1\ day^{-1}$). This suggests that most cells in the latent phase will be converted to an active state and produce progeny virions before they will undergo natural cell death.[77]

Finally, when the latent phase models were compared with the reference model, we found that there was little or no change in the qualitative behavior of the model. For example, there was only one maximum observed in the viral load in both reference and latent phase models. As in the reference model, free virions in the latent phase model were not completely cleared within 6-8 days ($\sim 10^8$ virions remained at 10 days post infection, which is an order of magnitude greater than the initial viral load). Furthermore, in both the reference and latent phase models, more than 90% of susceptible cells are exhausted within 5 days post infection. Clearly, even though significant quantitative differences were observed between the latent phase models and the reference model, the qualitative behaviors of time courses for susceptible cells, free virions, and infected cells are unchanged. This creates a challenge in discriminating between the existence and absence of a latent phase on the basis of model fitting to viral load data alone.

4. NATURAL KILLER CELL MODEL (MODEL 3)

4.1. Introduction

Here we introduce a model which is again target-cell-limited, but contains a simple mechanism for innate immune response [Figure 13]. We adopt assumptions (i) to (vi) stated for the reference model chapter 2 and we use the same parameter values for β, ρ, ϕ, and χ. We add to this the following assumptions regarding natural killer cell activity in order to obtain Equations 13 through 16, and introduce parameters ε, α, and ψ.

i. Natural killer cells attempt to control infection by eliminating infected cells. The rate of infected cell killing by natural killer cells can be described by mass action kinetics with rate constant ε $cell^{-1}day^{-1}$, which will be referred to as a destruction parameter.

ii. The activation of natural killer cells is assumed to be modulated by the presence of infected cells. The dependence on I is first order with rate constant α day^{-1}.

iii. The half-life of natural killer cells is assumed to be 10 days. Decay of natural killer cells is governed by rate constant ψ day^{-1}.

iv. The model parameters and initial conditions are outlined in the TABLE III and TABLE IV, respectively.

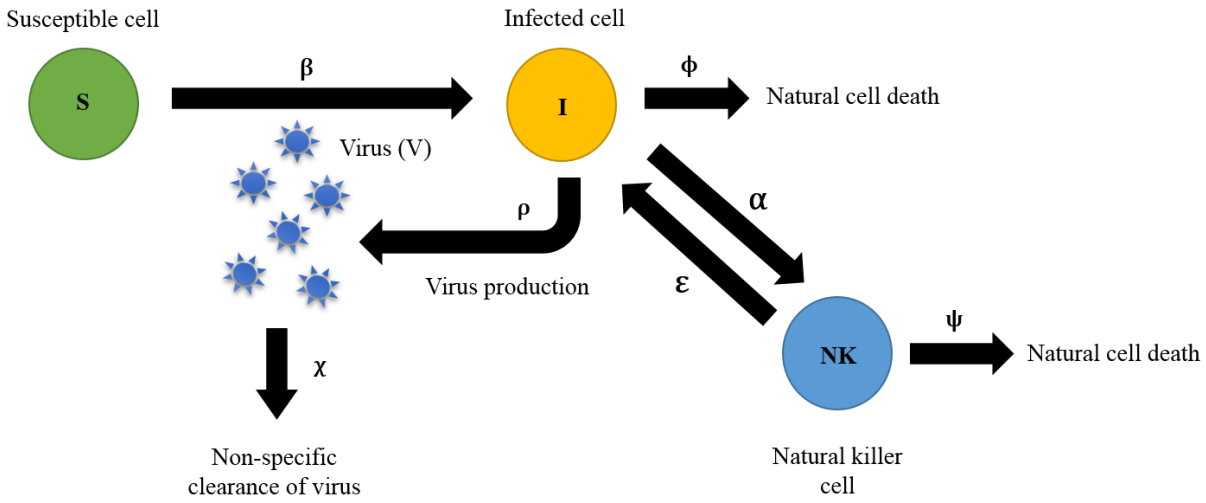

Figure 13. Schematic representation of the natural killer cell model.

$$\frac{dS}{dt} = -\beta[S][V] \quad [13]$$

$$\frac{dI}{dt} = \beta[S][V] - \phi[I] - \varepsilon[I][N] \quad [14]$$

$$\frac{dN}{dt} = \alpha[I] - \psi[N] \quad [15]$$

$$\frac{dV}{dt} = \rho[I] - \chi[V] \quad [16]$$

TABLE III. Parameters values for equations given in Equations 13 through 16.

Model Parameters	**Value**	**Units**	**Reference**
Infection rate (β)	10^{-10}	virion^{-1} day^{-1}	76
Natural death of infected cells (ϕ)	1	day^{-1}	76
Production of free virus (ρ)	340	cell^{-1} day^{-1}	76
Non-specific clearance of free virus (χ)	2	day^{-1}	76
Activation of NK cells (α)	0.52	day^{-1}	78
Natural death of NK cells (ψ)	0.07	day^{-1}	68,69
Action of NK cells on infected cells (ε)	10^{-10}	cell^{-1} day^{-1}	See text

TABLE IV. Initial conditions for equations given in Equations 13 through 16.

Initial Conditions	**Value**	**Units**	**Reference**
Susceptible cells (S_0)	10^9	cells	76
Infected cells (I_0)	0	cells	76
Free virus (V_0)	10^7	virions	76
NK cells (N_0)	0	cells	78

4.2.<u>Results and Discussion</u>

Susceptible cells (S) are rapidly infected, giving rise to infected cells (I). This increase in the population of infected cells generates new free virions (V) and triggers the activation of natural killer cells. At first, we assumed the value of the destruction parameter (ε) to be 10^{-10} cell^{-1}day^{-1}, which is equal to the rate of T-cell response described in Chang and Young. [76] We chose this initial value because both natural killer cells and T-cells act by hastening the death of infected cells.

However, the viral dynamics observed using this parameter value was found to be indistinguishable from the reference model [Figure 14]. This would imply that the natural killer cell response is ineffective in controlling the infection; in other words, $\varepsilon = 10^{-10}$ cell^{-1} day^{-1} is not large enough to make the natural killer cell response effective. Therefore, we sought to examine the physiologically reasonable limits of this destruction parameter by calculating the viral load as a function of time for a range of values of ε.

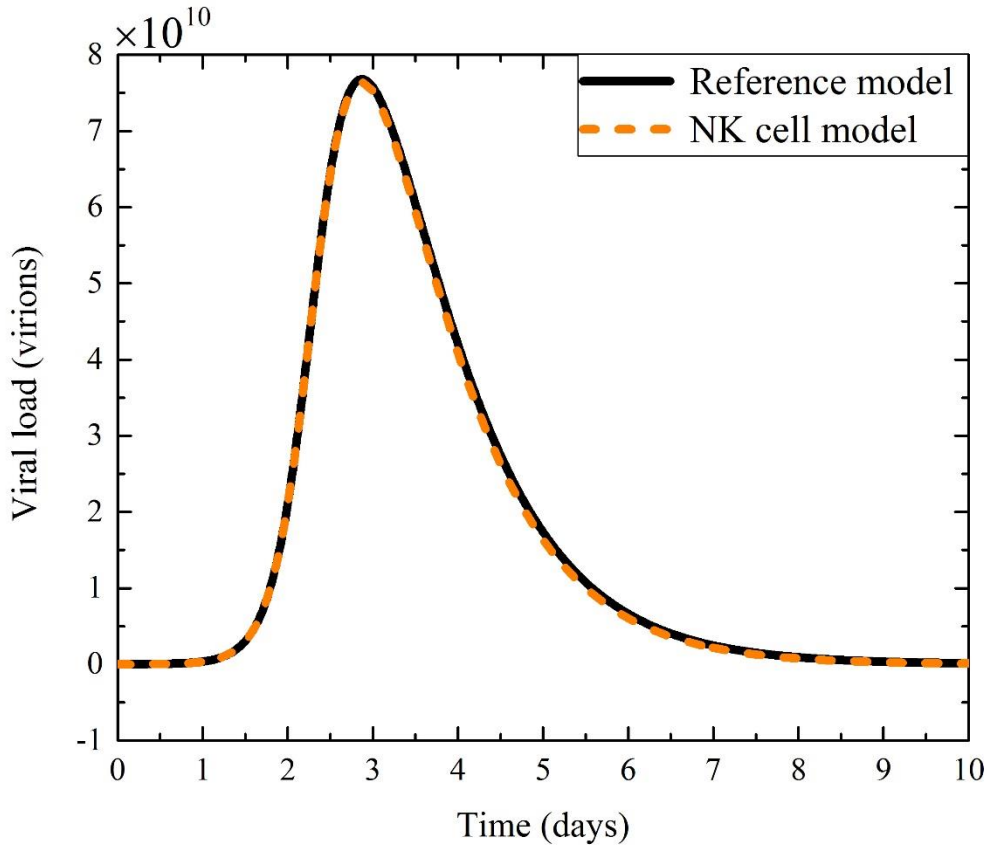

Figure 14. Comparing the viral loads between reference model (solid black line) and natural killer cell model (dashed orange line) for $\varepsilon = 10^{-10}$ cell^{-1} day^{-1}.

4.2.1. Examining the Valid Range of the Destruction Parameter

At the maximum in the time course for the population of infected cells, the following relationship can be derived from Equation 14.

$$I_{max} = \frac{\beta SV}{\phi + \varepsilon N} \quad [17]$$

Here, the denominator represents two death mechanisms for infected cells, one natural, ϕ, and one mediated by the immune response, εN. We therefore consider two limiting cases: (i) $\boldsymbol{\phi \gg \varepsilon N}$ and (ii) $\boldsymbol{\phi \ll \varepsilon N}$. When $\phi \gg \varepsilon N$, Equation 17 reduces to $I_{max} = \frac{\beta SV}{\phi}$ which is same result obtained for the reference model. On the other hand, when $\phi \ll \varepsilon N$, then Equation 17 reduces to $I_{max} = \frac{\beta SV}{\varepsilon N}\Big|_{t(I_{max})}$. If the number of susceptible cells (S) and natural killer (N) cells were of similar magnitude, then for $\beta = 10^{-10}$ virion^{-1} day^{-1} and $\varepsilon = 10^{-10}$ cell^{-1} day^{-1}, the maximum number of infected cells would have to be of similar order to the viral load. With each infected cell producing hundreds of free virions, this is not valid. For a robust natural killer cell effect, either the value of ε should be greater than 10^{-10} cell^{-1} day^{-1} or the natural killer cell population should far exceed the population of susceptible cells.

The case of $\varepsilon = 10^{-10}$ cell^{-1} day^{-1} represents a worst case scenario wherein the innate immune response makes no difference to physiological outcomes. We can use this case to estimate maximum activation of the natural killer cell population, as this term is dictated only by the population of infected cells, which will adopt its maximum value when natural killer cells fail to execute their role. We find the maximum natural killer cell count to be 1.57×10^{8} cells. Reconsidering Equation 17, we propose that for natural killer cell response to take effect, the term εN should at least be equal to the natural cell death rate constant (ϕ). Thus, the lower limit of the destruction parameter (ε) can be taken as 10^{-8} cell^{-1} day^{-1}. To find a corresponding upper limit the following analysis was performed.

Considering the viral load (7.68×10^{10} virions) observed for $\varepsilon = 10^{-10}$ cell^{-1} day^{-1} as a reference value, the parameter ε was increased until a 99% reduction in the maximum viral load was observed in which case, we found $\varepsilon = 10^{-5}$ cell^{-1} day^{-1} [Figure 15 and TABLE V].

TABLE V. Percentage decrease in maximum viral load as a function of destruction parameter.

Destruction parameter ε (cell^{-1} day^{-1})	**% decline in V_{max}**
10^{-10}	0
10^{-9}	5
10^{-8}	30
10^{-7}	72
10^{-6}	95
10^{-5}	99

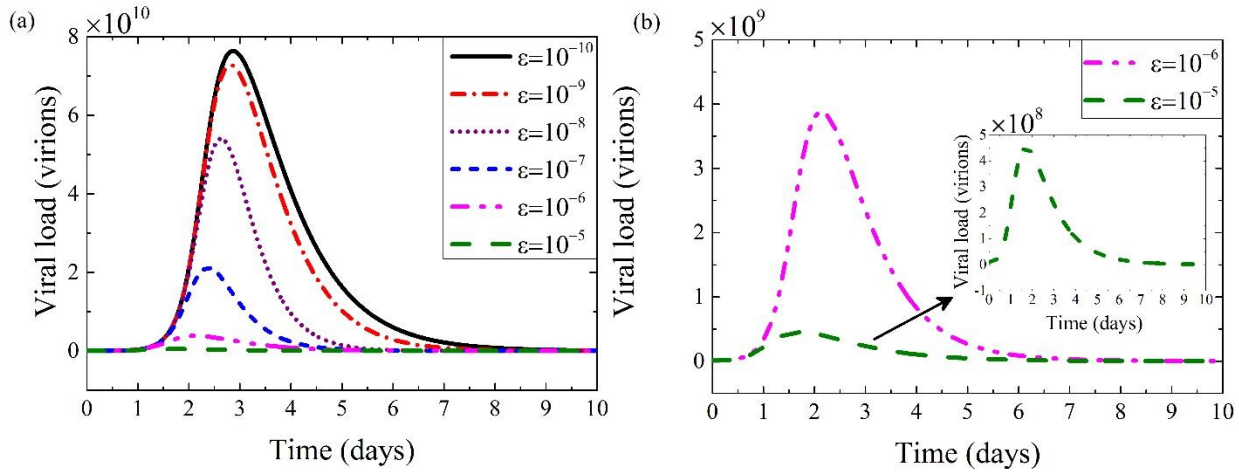

Figure 15. Viral load as a function of the destruction parameter (ε): (a) $\varepsilon = 10^{-10}$ cell^{-1} day^{-1} to 10^{-5} cell^{-1} day^{-1}, (b) $\varepsilon = 10^{-6}$ cell^{-1} day^{-1} to 10^{-5} cell^{-1} day^{-1}. Viral load for $\varepsilon = 10^{-5}$ cell^{-1} day^{-1} is zoomed in for more clarity (dashed green line).

We further examined the variation observed in the maximum viral load as a function of ε starting from the lower limit of $\varepsilon = 10^{-8}$ cell^{-1} day^{-1} to the upper limit of $\varepsilon = 10^{-5}$ cell^{-1} day^{-1} by collecting more data between these limits [Figure 16]. The relationship between parameter ε and the decline in the maximum viral load was found to fit the following equation:

$$\frac{\%\ \text{decrease in}\ V_{max}}{V_{limit}} = \frac{\varepsilon^n}{k^n + \varepsilon^n} \qquad [18]$$

Where, $V_{limit} = 100$ was fixed, and the constants $n = 0.82$ and $k = 3.04\times10^{-8}$ cell^{-1} day^{-1} were estimated by fitting the data [Figure 16].

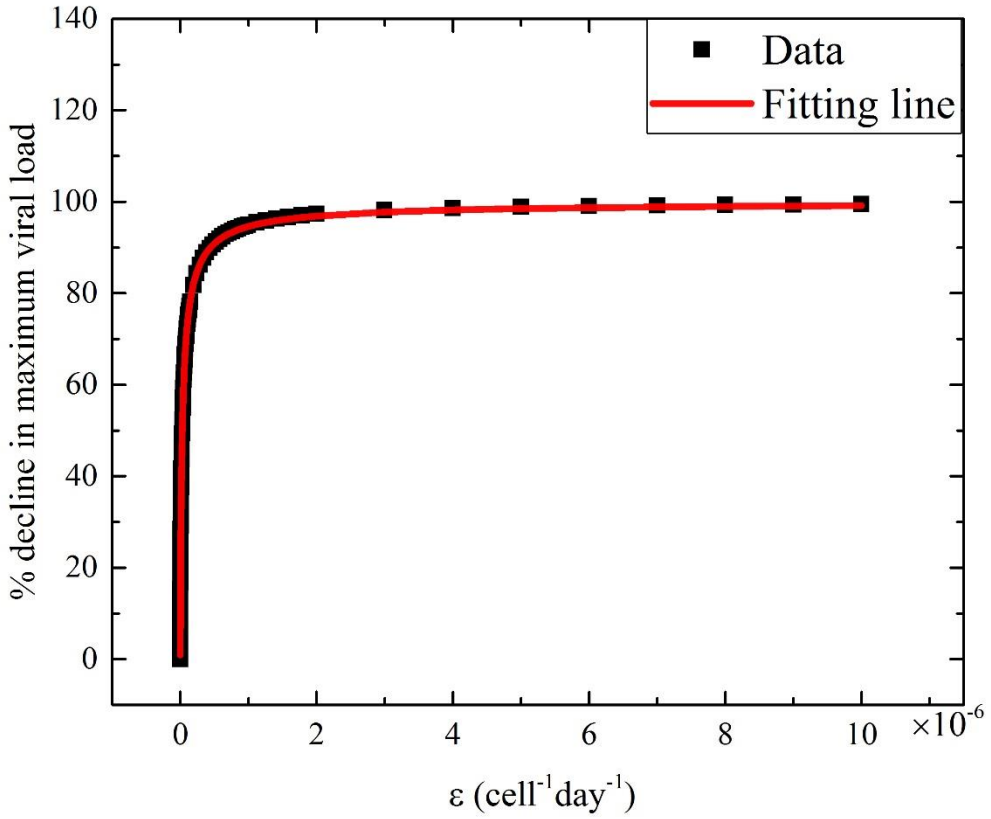

Figure 16. Percentage of decline in maximum viral load with respect to destruction parameter ε.

4.2.2. Estimation of Physiologically Relevant Range for Destruction Parameter (ε)

To predict a physiologically relevant range of the parameter ε, two different model outcomes were compared with experimental observations reported in the literature. For typical influenza infection in humans, experimental studies suggest that a maximum in viral load is achieved between 2-3 days post infection[79-85], and the maximum natural killer cell activity is observed after 3-4 days.[60,71] The model results for $\varepsilon = 10^{-8}$ cell^{-1} day^{-1} to 10^{-6} cell^{-1} day^{-1} were found to be consistent with the above experimental findings [Figure 15 and Figure 17]. Therefore, values

of this parameter between 10^{-8} and 10^{-6} $cell^{-1}$ day^{-1} should be physiologically valid. This corresponds to a 30-95% reduction in maximum viral load.

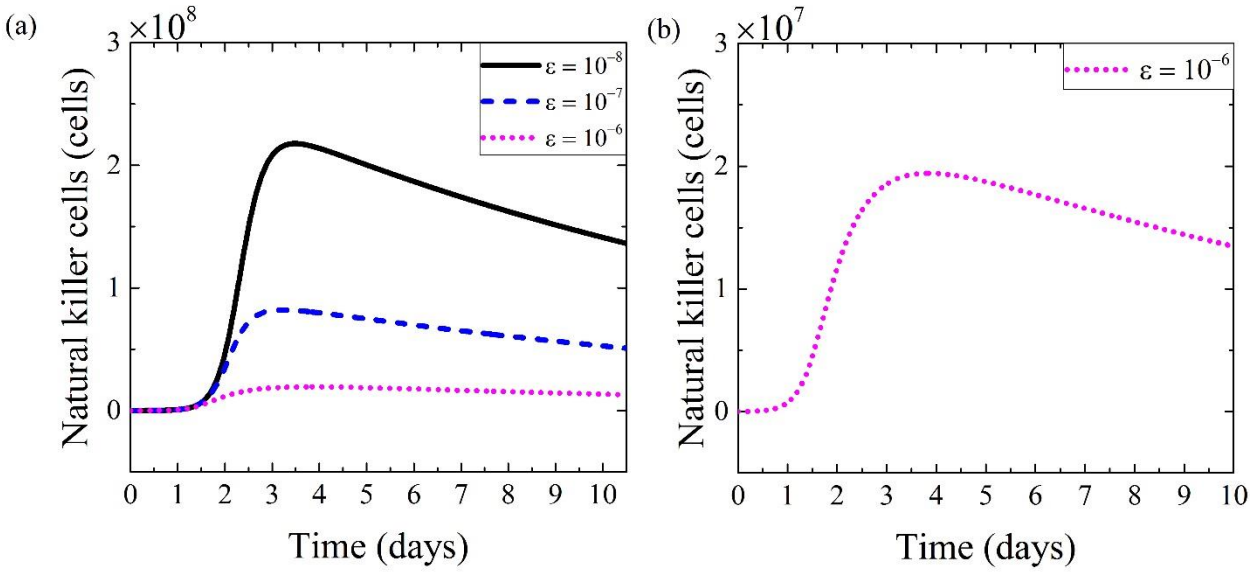

Figure 17. Activity of natural killer cells as a function of ε: (a) ε = 10^{-8} to 10^{-6} $cell^{-1}$ day^{-1} , (b) ε =10^{-6} $cell^{-1}$ day^{-1}.

As seen in Figure 17, the number of natural killer cells decreases with an increase in the value of the destruction parameter ε. It stands to reason that the more effective natural killers are at eliminating infected cells, the fewer natural killer cells are required to control the influenza infection. From the above discussion it is clear that an effective natural cell response should efficiently control the early stages of infection.

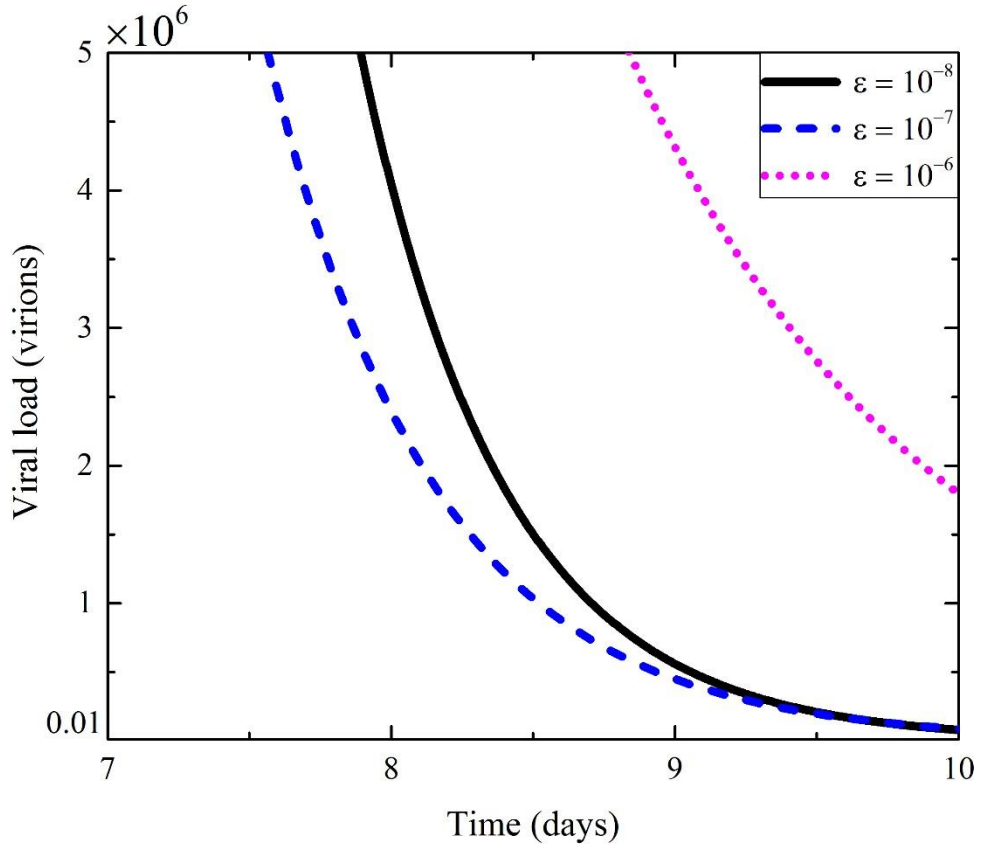

Figure 18. Viral load as a function of the destruction parameter ε (from 10^{-8} to 10^{-6} $cell^{-1}$ day^{-1}).

Although the infection is controlled during the initial phase, we find that the natural killer cell response model is insufficient to explain the resolution of typical influenza infection within the physiologically valid timeline (6-8 days post infection) [79-85] [Figure 18]. The unresolved infection could be due to two interrelated reasons:

i. There is no specific immune component in the model to clear free virions, hundreds of which are being generated by each infected cell.

ii. An effective natural killer cell response prolongs the availability of susceptible cells, and these cells become infected by the persistent free virions [Figure 19].

Therefore, we model a specific component of adaptive immune response to remove the free virions in the next section.

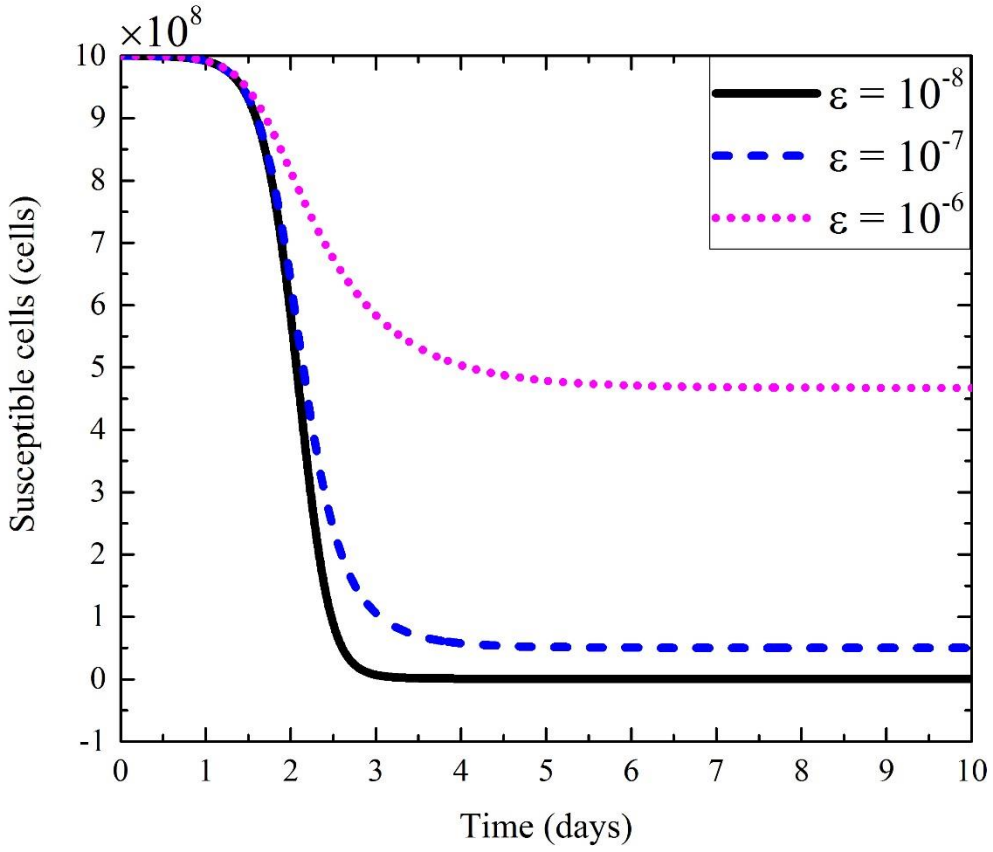

Figure 19. Population of susceptible cells as a function of parameter ε.

4.2.3. Model 4: Addition of Antibody Response to Natural Killer Cell Model

The natural killer cell response is insufficient, as modeled, to prevent eventual infection of all susceptible cells. This is a logical consequence of the fact that this mechanism of innate immunity only addresses the population of infected cells. Cell lysis is only partially effective at controlling infection when each cell has the capacity to produce hundreds of virions. Complete clearance of the virus is facilitated by a mechanism that directly hastens the clearance of free virus particles. Antibodies, proteins that arise as part of the adaptive immune response, can neutralize and facilitate the clearance of virions. Antibody formation is a feature of the humoral (or B-Cell) response. Activated B-cells secrete antibodies within a few days post infection. The antibodies bind with influenza virions, inhibiting their ability to contact surface receptors on cells as required for cell entry. In addition the antibody-coated surface marks the virion for clearance.[86,87]

While cytotoxic T-cells are also an important component of adaptive immunity, they function similarly to natural killer cells in that they cause infected cell death. In adding an adaptive immune component to our model, we chose to consider an antibody-like response, as a means of directly impacting the population of free virions. Unlike natural killer cells in which the maximum activity is observed within 5 days post infection, both T-cell and antibody responses become evident only after 5 days post infection. With this understanding of the physiology, we attempt to model a simple antibody response with the following assumptions:

i. The number of antibody molecules is proportional to number of B-cells, hence only one of these populations need be explicitly represented in the model.

ii. Before the onset of infection, the antibody population is negligible (as when the host has no prior exposure to the specific influenza strain).

iii. The activation of antibodies is proportional to the population of free virions with rate constant τ day^{-1}.

iv. Once activated, antibodies stimulate expansion of their own population with rate constant $\sigma = 1$ day^{-1}. [52]

v. Antibody-mediated clearance of free virions can be described as mass action kinetics with rate constant $\kappa = 1$ $cell^{-1}$ day^{-1}. [52]

Experimental studies show that antibodies specific to influenza infection can be detected even after 10 days post infection.[87-89] Consequently, we can neglect the natural clearance of antibodies in our model, which is aiming for validity only to the point of viral clearance (6-8 days for typical influenza infection).

To the natural killer cell model, we now add Equation 19, which describes the dynamics of antibody activation and proliferation. We also modify the ODE for free virions to include an antibody-mediated clearance term [Equation 20].

$$\frac{dA}{dt} = \tau[V] + \sigma[A] \quad [19]$$

$$\frac{dV}{dt} = \rho[I] - \chi[V] - \kappa[V][A] \quad [20]$$

We based our initial estimate of the antibody activation parameter ($\tau = 10^{-9}$ day^{-1}) on that observed in a study of IAV infection in mice[59]. As all other parameters in our model are valid for influenza infection in humans, we have attempted herein to estimate a valid range of values for this activation parameter (τ) in humans. In establishing validity, we use the following criteria: (i) typical influenza infection is resolved within 8 days [79-85]; (ii) maximum in viral load should occur between days 2 and 3 [79-85]; (iii) maximum natural killer cell activity should occur between 3 and 4 days. [60,71]

Our fourth model combines both an innate (natural killer cell) and an adaptive (antibody) response mechanism. Although one of these is nominally active 'early' in infection and the other 'late' in the course of infection, there is likely to be an interaction between these two infection-controlling mechanisms. Thus, our prior determination of a valid range for natural killer cell activity may need reconsidering. We chose to begin our interrogation of antibody activity by employing the previously determined physiologically valid range of values for ε, the index of natural killer cell cytotoxicity (i.e., $\varepsilon = 10^{-8}$ to 10^{-6} cell^{-1} day^{-1}). By this we will be able to analyze different scenarios starting from a strong natural killer cell activity to weak natural killer activity. We chose to model the antibody response coupled with three different values of the natural killer cell destruction parameter: $\varepsilon = 10^{-6}$ (strong response), 10^{-7} (moderate response), and 10^{-8} (weak response) cell^{-1} day^{-1}. For this we first have to define the number of virions that corresponds to the resolution of infection. In experimental studies conducted in human volunteers during influenza infection the resolution of infection is defined as viral load between 1-10 $TCID_{50}$/mL of nasal wash. [79-85] There is no accurate estimate for conversion of $TCID_{50}$/mL to virus particles, so we

choose to employ herein the approximations presented by Handel et al. [52], wherein this measure of viral load in nasal wash is said to correspond to 10^2-10^5 virus particles at the site of infection. Henceforth, we will define resolution of the infection as a reduction in viral load to 100 virions.

We begin our interrogation of antibody-mediated resolution by considering a scenario where natural killer cell cytolytic activity tuned to $\varepsilon = 10^{-6}$ cell^{-1} day^{-1}, which corresponds to a relatively strong innate immune response. We set $\tau = 10^{-9}$ day^{-1}, the initial antibody activation value obtained from experiments on mice. First, we increased the value of the antibody activation parameter by 4 orders of magnitude to 10^{-5} day^{-1}. We found that for $\tau = 10^{-9}$ day^{-1} or above, virion clearance was achieved within four days post infection, which is more rapid than desired given that the antibody response is part of adaptive immunity and is not expected to be effective before ~5 days post infection. Hence, we chose $\tau = 10^{-10}$ day^{-1} as upper limit and decreased this value by 3 orders of magnitude to 10^{-13}. Clearance of the virus (≤100 virions) was achieved within 8 days only for values of τ between 10^{-10} and 10^{-11} day^{-1} [Figure 20].

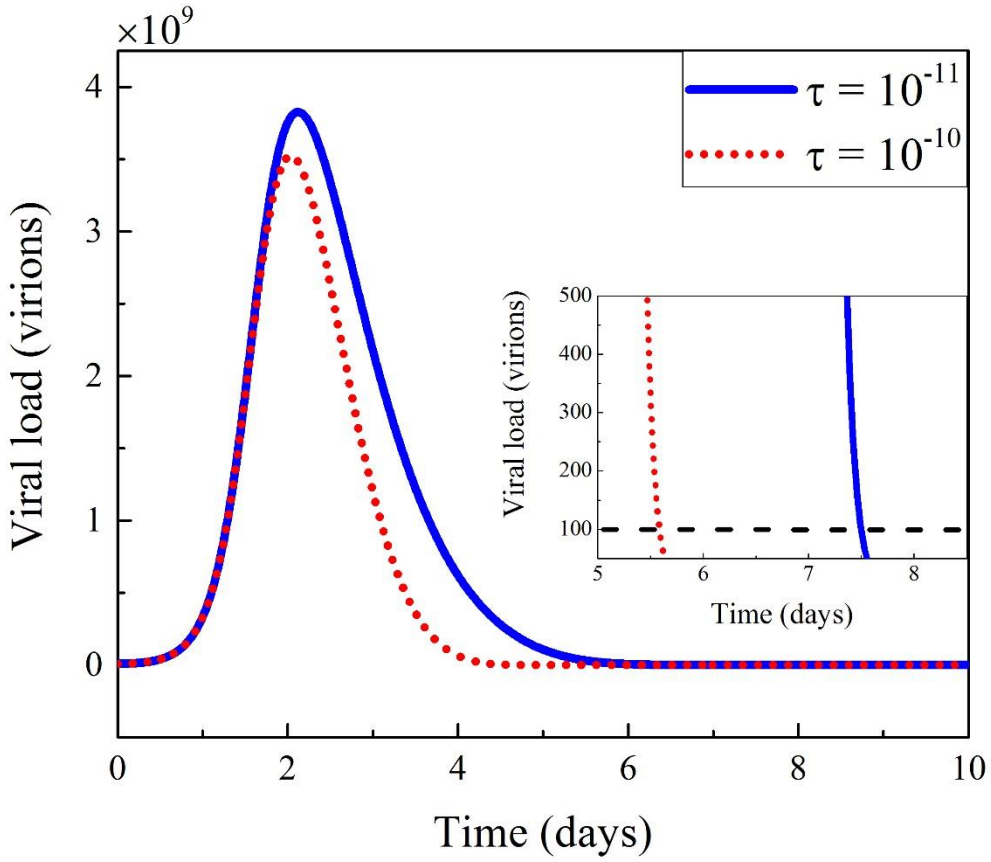

Figure 20. Viral load for different values of antibody activation parameter τ; $\varepsilon = 10^{-6}$ cell^{-1} day^{-1}.

We followed a similar procedure for analyzing the effect of antibody activation on virus clearance for the case of a moderate innate immune response ($\varepsilon = 10^{-7}$ cell^{-1} day^{-1}). Again starting from the initial guess of $\tau = 10^{-9}$ day^{-1}, we increased this value by four orders of magnitude. We found that for τ greater than or equal to 10^{-8} day^{-1}, the maximum viral load was achieved within 2 days post infection, which is faster than desired. Thus, $\tau = 10^{-9}$ day^{-1} was taken as the upper limit for this case. To estimate a lower limit, τ was decreased from 10^{-9} day^{-1} (initial value) to 10^{-13} day^{-}

[1]. The virus was cleared within 8 days post infection for values of 10^{-9} day^{-1} to 10^{-11} day^{-1}. Also, maximum viral load and maximum natural killer cell activity were found to occur around 2-3 days post infection[79-85] and 3-4 days post infection[60,71], respectively. As all these model outcomes were found to be consistent with the physiological observations, $10^{-11} < \tau < 10^{-9}$ day^{-1} can be considered a valid range for the antibody activation parameter during a moderate natural killer cell response [Figure 21].

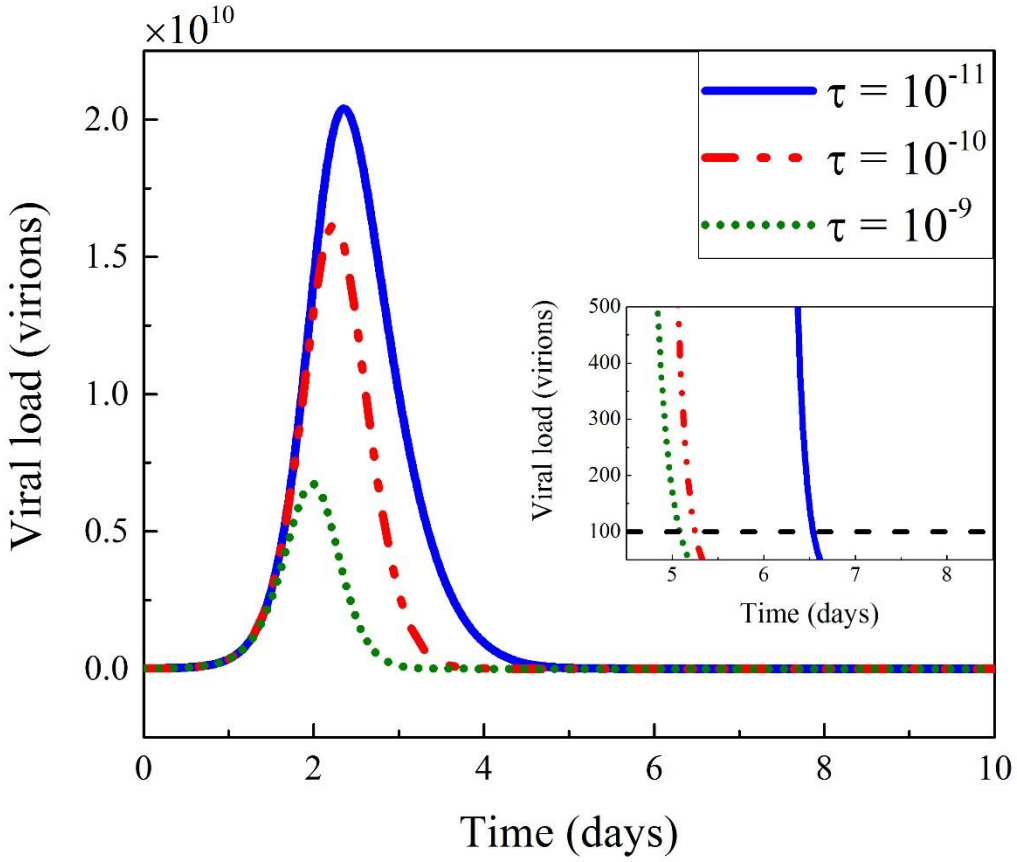

Figure 21. Viral load for different values of antibody activation parameter τ; $\varepsilon = 10^{-7}$ $cell^{-1}$ day^{-1}.

Finally, we consider the antibody effect on free virions for the case of a weak innate immune response ($\varepsilon = 10^{-8}$ cell^{-1} day^{-1}). We found that for $\tau \geq 10^{-8}$ day^{-1}, the maximum in viral load was occurred too early (≤ 1.5 days post infection). Thus, we assigned an upper limit for this case of $\tau = 10^{-9}$ day^{-1}. Then we decreased the value of τ by four orders of magnitude. Virions were successfully cleared (≤100 virions) within 8 days for $2\times10^{-11} \leq \tau \leq 10^{-9}$ day^{-1} [Figure 22]. The time to maximum viral load and the time of maximum natural killer cell activity also compared favorably with the established time course of typical influenza infection. Hence, $2\times10^{-11} \leq \tau \leq 10^{-9}$ day^{-1} can be considered as appropriate to produce a typical time course of infection for the case of weak natural killer cell activity ($\varepsilon = 10^{-8}$ cell^{-1} day^{-1}).

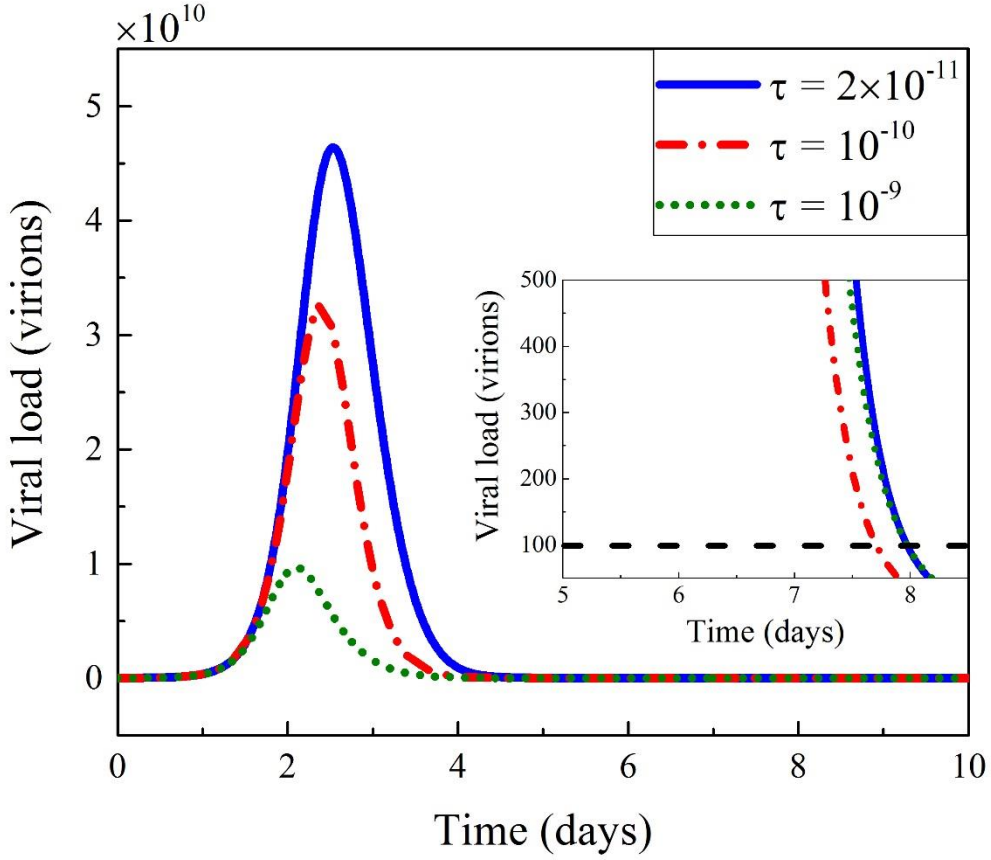

Figure 22. Viral load for different values of activation parameter τ; ε = 10^{-8} $cell^{-1}$ day^{-1}.

TABLE VI. Timing of critical events over the course of simulated influenza infection, as predicted in model 4.

Destruction parameter of NK cells ($cell^{-1}$ day^{-1})	**Activity parameter of antibodies (τ) (day^{-1})**	**Maximum viral load (days)**	**Time of virus clearance (days)**	**Maximum activity of NK cells (days)**
$\varepsilon = 10^{-6}$	10^{-11}	2	7-8	3
	10^{-10}	2	5-6	4
$\varepsilon = 10^{-7}$	10^{-11}	2	7-8	3
	10^{-10}	2	5-6	3
	10^{-9}	2	5-6	3
$\varepsilon = 10^{-8}$	2×10^{-11}	2	7-8	3
	10^{-10}	2	7-8	3
	10^{-9}	2	7-8	3

The results for different ε and τ, along with the model outcomes, are given in TABLE VI. The antibody response has little effect on the time to maximum viral load. However, antibody response has a significant effect on the clearance of free virions. The time at which virions are predicted to be completely cleared varies from 5-8 days post infection. Also, we note that when innate immune response is strong ($\varepsilon = 10^{-6}$ $cell^{-1}$ day^{-1}), a less robust adaptive immune response (10^{-11} $day^{-1} < \tau < 10^{-10}$ day^{-1}) is sufficient to clear the virus [TABLE VI].

TABLE VII. Percentage decrease in maximum viral load as a function of activity parameter.

Destruction parameter of NK cells ($cell^{-1}$ day^{-1})	**Activity parameter of antibodies (τ) (day^{-1})**	**% decline in V_{max} compared to reference model**	**% decline in V_{max} compared to NK cell model**
$\varepsilon = 10^{-6}$	10^{-11}	95	1
	10^{-10}	95	9
$\varepsilon = 10^{-7}$	10^{-11}	73	4
	10^{-10}	79	24
	10^{-9}	91	68
$\varepsilon = 10^{-8}$	2×10^{-11}	39	14
	10^{-10}	57	40
	10^{-9}	87	82

While not altering the time to maximum, antibody-mediated viral clearance does alter the predicted maximum viral load. TABLE VII compares the decline in the maximum viral load (V_{max}) in the antibody model to that in the reference and natural killer cell models. It is clear that increasing the antibody activation parameter decreases the V_{max}. However, the relative importance of the innate and adaptive immune mechanisms differs as a function of the strength of the innate response. There is a trade-off between the two defense mechanisms. When the innate response is strong, the reduction in peak viral load is attributable almost entirely to natural killer cell activity. Likewise, when the natural killer cell response is relatively weak, the decline in viral load is almost entirely attributable to the role of the antibody response.

Figures 23-25 show the antibody response for τ and ε values given in TABLE VI. The antibody population begins to rise after 4-5 days post infection. It increases 10^2-10^4 fold by 6-8 days post infection. The model results for antibody response were found to be consistent with both experimental observation and also with the previous modeling work of influenza infection in humans. [54, 95].

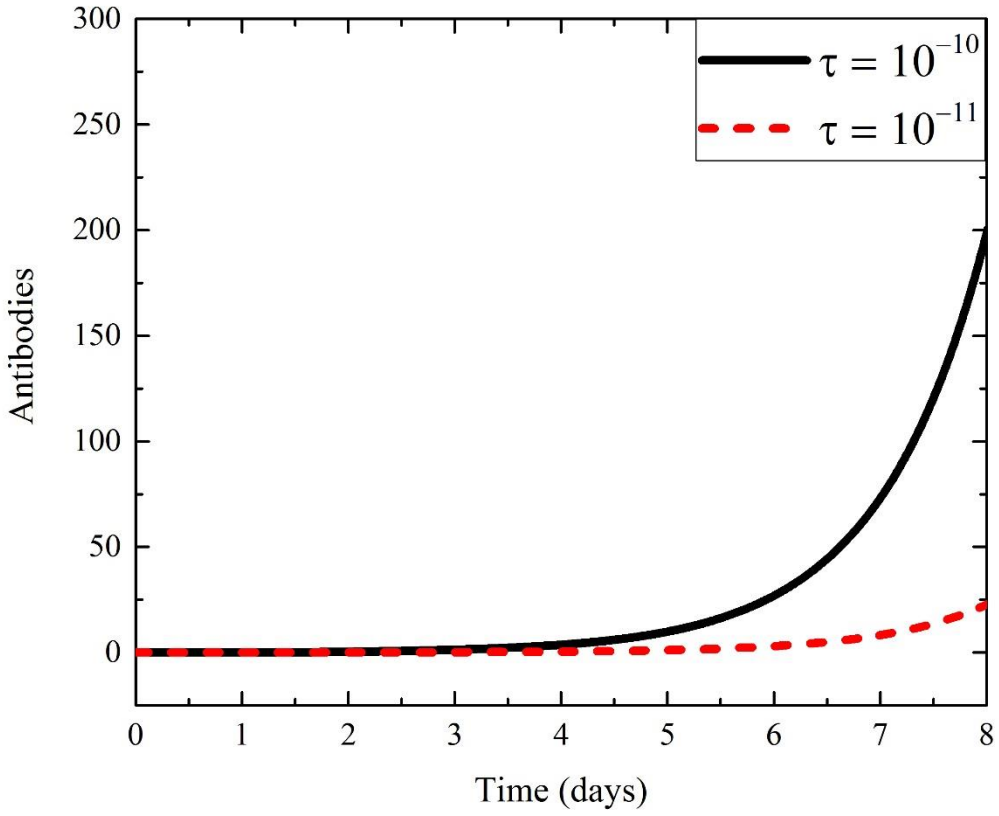

Figure 23. Antibody response for different values of activation parameter τ; ε = 10^{-6} $cell^{-1}$ day^{-1}.

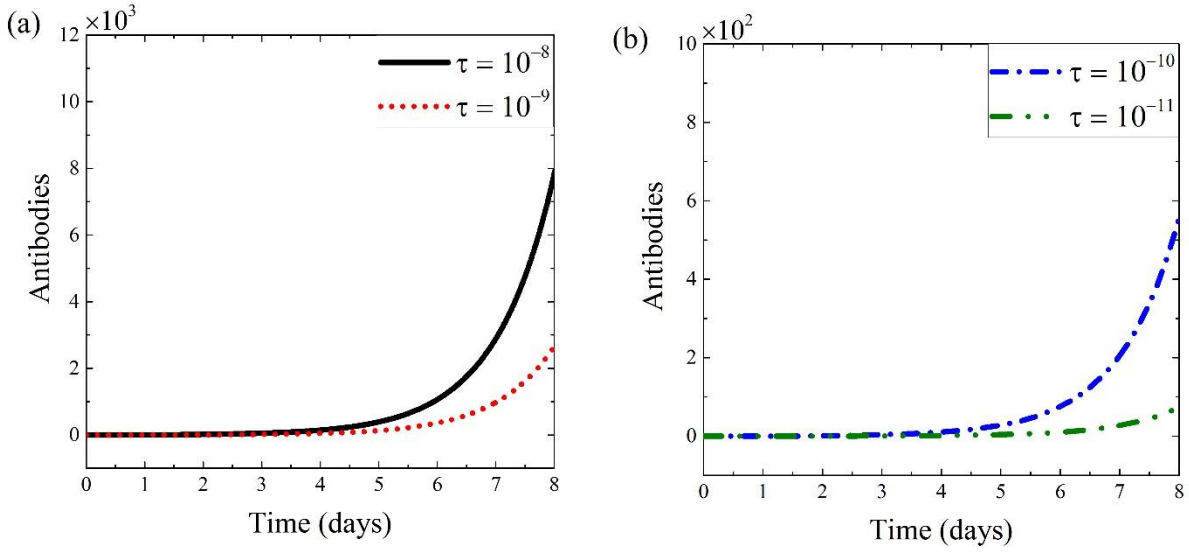

Figure 24. Antibody response for different values of activation parameter τ; ε = 10^{-7} $cell^{-1}$ day^{-1}.

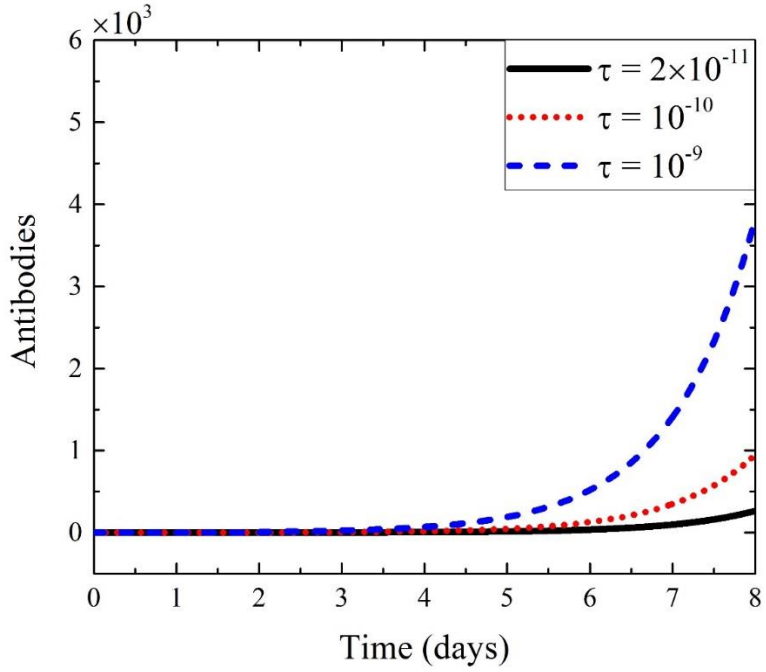

Figure 25. Antibody response for different values of activation parameter τ; ε = 10^{-8} $cell^{-1}$ day^{-1}.

4.3. Summary and Conclusions

The effect of innate immunity on influenza viral dynamics was interrogated using a simple natural killer cell response model. One major barrier in the modeling of influenza infection in humans is a lack of experimental data for cytokines and other immune response factors. Here we adopt an alternative approach to characterizing a plausible range for the parameter governing natural killer cell cytolytic activity (ε). A suitable range for this parameter was estimated by comparing model outcomes with known physiology. In addition to this, a theoretical relationship between the destruction parameter (ε) and reduction in percentage of the maximum viral load (V_{max}) was estimated. A strong natural killer cell response results in effective lysis of infected cells, hence virus production inside the host is reduced. While the simulated natural killer cell response proves to be effective in controlling the initial phase of infection (reducing viral load by 30-95%), it does not by itself resolve the infection. A prolonged reservoir of free virions allows for continued infection of susceptible cells within the host. Hence, it was necessary to introduce another component of immune response to enable resolution of the infection in the physiologically reasonable timeframe of 7-8 days.

When a simple antibody-based adaptive immune response was incorporated into the natural killer cell response model, appropriate parameter ranges were found to allow complete resolution of the infection. As the activation parameter for this simple model of antibody response had not been established in the literature for influenza infection in humans, we used three model outcomes (time to maximum viral load, time to maximum natural killer cell activity, and time to complete virion clearance) as our basis for selecting a valid range of values for this parameter. Irrespective

of the robustness of natural killer cell response (weak, moderate or strong), the physiologically plausible range for the antibody activation parameter can be taken to be from 10^{-11} to 10^{-9} day^{-1}. We note here that these ranges were determined for fixed values of the remaining model parameters and acknowledge that many of these parameters are characterized by their own broad physiological ranges.

5. SUMMARY AND CONCLUSIONS

In the present work, a within-host viral kinetic modeling approach was used to depict influenza infection in humans. Simple target-cell-limited models were built with increasing complexity, starting from a simple reference model (chapter 2) with three variables and four parameters. In the next chapter (chapter 3) we performed a comparative study to determine the relevance of natural death of infected cells existing in a latent phase. A model without this term resulted in a higher population of infected cells (both latent and active), and higher viral load. While, biologically, it is clear that cells in the latent phase can die, the impact cell death has on the model outcome depends on the relative values of rate constants dictating the conversion of latently infected cells to the active phase (γ) and the natural rate of cell death (ϕ). Hence, the relevance of the natural cell death term in the context of latently infected cells depends on the duration of that phase for the specific virus of interest. In order to minimize the number of model parameters, death of latent cells should be included if the time spent in the latent phase approaches the cell lifetime. However, this may need to be known a *priori*, as the qualitative nature of the time courses does not change in the presence or absence of the cell death term or in the presence or absence of a latent cell population. Discrimination between these biological mechanisms may not be clear from simple data fits to experimentally determined viral load.

A component of innate immune response, natural killer cells, is modeled in chapter 4. Most of the modeling studies performed so far have attempted to model only interferon production as the mechanism of innate immunity. Recent literature suggests that natural killer cells are critical mediators of the innate immune response during influenza infection. This is a first attempt to

explicitly model natural killer cell population within a minimal framework. Here, we did not include interferon response to avoid two additional parameters and one additional variable. The physiological range the parameter governing natural killer cell cytolytic activity (ε) was estimated using a quantitative analysis with performance criteria based on the known physiology of typical influenza infection in humans. The appropriate range was found to be between 10^{-8} to 10^{-6} $cell^{-1}$ day^{-1}. Also, a theoretical relationship between this parameter (ε) and reduction in the maximum viral load (V_{max}) was presented. The maximum activity of natural killer cells was predicted to occur at ~3 days post infection for all cases ($\varepsilon = 10^{-8}$ to 10^{-6} $cell^{-1}$ day^{-1}).

Finally, an antibody response was added to the natural killer cell response model to mediate accelerated elimination of free virions. This was necessary to achieve a model outcome consistent with the experimentally observed duration of influenza viral load. As in the case of our natural killer cell model, the antibody based immune response model was constructed with a minimum set of parameters based on a mechanistic framework capturing specific assumptions about the underlying biology. An initial guess for the parameter governing antibody activation was taken from a mathematical model of H1N1 infection in mice. A range of alternative values was then estimated to obtain an evolution of host and pathogen dynamics that is consistent with a range of activity for the natural killer cell response.

While a robust natural killer cell response was required to control growth of the free virions population, the antibody response facilitates termination of the infection. A robust antibody response coupled with a weaker natural killer cell response was observed to achieve the same

outcome as a robust natural killer response and a more moderate antibody response – giving a clear indication of the compensatory nature of host immune mechanisms. It is this compensatory nature that makes it difficult to tease apart the detailed biological mechanisms of immunity from scarce data addressing only the relatively easily quantified measure of viral load.

6. LIMITATIONS AND FUTURE WORK

Although we have biological evidence for natural killer cell activity and antibody responses, more data in terms of virus strain specific antibody activity, and natural killer cell activity is required for detailed quantitative analyses, especially in humans. Many experiments are performed on animals (e.g. mice, horses, ferrets) to understand the immune responses exhibited by these hosts during influenza infection, but how far these results can be extrapolated to characterize the infection within humans still remains questionable and unclear. Thus, shortcomings in the sources of biological data for specific immune players remains a limiting factor for modeling influenza infection in humans.

An important component of innate immunity, the natural killer cell response, was modeled with a minimum set of parameters. However natural killer cells are far from the sole mediator of innate immunity. Extending the current work with more than one component of innate immunity can help to clarify the necessity of adaptive immune responses in the presence of a strong innate immune response. Further, such models can be used to interrogate the kinetics of infection for influenza viral strains of varying infectivity and virulence (e.g. H3N2 virus of human origin, H5N1, H5N2 strains of avian origin). Likewise the effect of natural killer cell activity in the case of wild-type and mutant viruses can be investigated using a natural killer cell model. For example, there is evidence that the recent H3N2 (1996-2003) influenza virus could have undergone mutation to evade the natural killer cell response.[71]

CITED LITERATURE

1. PJ Imperato. Smallpox. The fight to eradicate a global scourge. J Community Health 2003;28:390.

2. JK Taubenberger, DM Morens. 1918 Influenza: the Mother of all Pandemics. Emerging Infectious Diseases 2006;12:15-22.

3. First Global Estimates of 2009 H1N1 Pandemic Mortality Released by CDC-Led Collaboration 2012.

4. Avian influenza A(H7N9) virus – China - Emergency Preparedness Response from World Health Organization (WHO), 2015.

5. Hepatitis C - Fact Sheet from World Health Organization (WHO), July 2015.

6. HIV - Fact Sheet from World Health Organization (WHO), November 2015.

7. Measles - Fact Sheet from World Health Organization (WHO), November 2015.

8. Ebola Viral Disease(EVD) - Fact Sheet from World Health Organization (WHO) January 2016, 2016.

9. Zika virus disease in the United States, 2015–2016, March 2016.

10. Global Health Observatory (GHO) HIV/AIDS data, April 2016.

11. T Vos, RM Barber, B Bell, A Bertozzi-Villa, S Biryukov, I Bolliger, et al. Global, regional, and national incidence, prevalence, and years lived with disability for 301 acute and chronic diseases and injuries in 188 countries, 1990-2013: a systematic analysis for the Global Burden of Disease Study 2013. Lancet 2015;386:743-800.

12. M Naghavi, H Wang, R Lozano, A Davis, X Liang, M Zhou, et al. Global, regional, and national age-sex specific all-cause and cause-specific mortality for 240 causes of death, 1990-2013: a systematic analysis for the Global Burden of Disease Study 2013. Lancet 2015;385:117-71.

13. WHO - Projections of mortality and causes of death 2015 & 2030, 2016.

14. Weekly U.S. Influenza Surveillance Report, March 2016.

15. Hamborsky J, Kroger A, Wolfe S. Epidemiology and Prevention of Vaccine-Preventable Diseases. 13th ed.: Washington D.C. Public Health Foundation; 2015.

16. C Fraser, CA Donnelly, S Cauchemez, WP Hanage, MD Van Kerkhove, TD Hollingsworth, J Griffin, RF Baggaley, HE Jenkins, EJ Lyons, T Jombart, WR Hinsley, NC Grassly, F Balloux, AC Ghani, NM Ferguson. Pandemic Potential of a Strain of Influenza A (H1N1): Early Findings. Science 2009;324:1557-61.

17. CE Mills, JM Robins, M Lipsitch. Transmissibility of 1918 pandemic influenza. Nature 2004;432:904-6.

18. KD Patterson, GF Pyle. The Geography and Mortality of the 1918 Influenza Pandemic. Bull Hist Med 1991;65:4-21.

19. FS Dawood, AD Iuliano, C Reed, MI Meltzer, DK Shay, P Cheng, D Bandaranayake, RF Breiman, WA Brooks, P Buchy, DR Feikin, KB Fowler, A Gordon, NT Hien, P Horby, QS Huang, MA Katz, A Krishnan, R Lal, JM Montgomery, K Molbak, R Pebody, AM Presanis, H Razuri, A Steens, YO Tinoco, J Wallinga, H Yu, S vong, J Bresee, MA Widdowson. Estimated global mortality associated with the first 12 months of 2009 pandemic influenza A H1N1 virus circulation: a modelling study. The Lancet Infectious Diseases 2012;12:687-95.

20. WHO-Global Vaccine Action Plan 2011-2020, 2016.

21. 2014-15 Seasonal Influenza Vaccine—Total Doses Distributed.

22. Flu Vaccine Nearly 60 Percent Effective, February 2016.

23. TG Sheu, VM Deyde, M Okomo-Adhiambo, RJ Garten, X Xu, RA Bright, EN Butler, TR Wallis, AI Klimov, LV Gubareva. Surveillance for neuraminidase inhibitor resistance among human influenza A and B viruses circulating worldwide from 2004 to 2008. Antimicrob Agents Chemother 2008;52:3284-92.

24. A Kelso, AC Hurt. Drug-resistant influenza viruses: why fitness matters. Nat Med 2012;18:1470-1.

25. Influenza (Seasonal) - Fact Sheet from World Health Organization (WHO) 2014:March.

26. CA Biron. Role of early cytokines, including alpha and beta interferons (IFN-alpha/beta), in innate and adaptive immune responses to viral infections. Semin Immunol 1998;10:383-90.

27. DL Brassard, MJ Grace, RW Bordens. Interferon-alpha as an immunotherapeutic protein. J Leukoc Biol 2002;71:565-81.

28. I Julkunen, T Sareneva, J Pirhonen, T Ronni, K Melen, S Matikainen. Molecular pathogenesis of influenza A virus infection and virus-induced regulation of cytokine gene expression. Cytokine Growth Factor Rev 2001;12:171-80.

29. S Ludwig, S Pleschka, T Wolff. A fatal relationship - Influenza virus interactions with the host cell. Viral Immunol 1999;12:175-96.

30. Chapter 7 - Antigen Processing and Presentation. In: Mak TW, Jett MESD, editors. Primer to the Immune Response (Second Edition), Boston: Academic Cell; 2014, p. 161-179.

31. Chapter 9 - T Cell Development, Activation and Effector Functions. In: Mak TW, Jett MESD, editors. Primer to the Immune Response (Second Edition), Boston: Academic Cell; 2014, p. 197-226.

32. Chapter 8 - The T Cell Receptor: Proteins and Genes. In: Mak TW, Jett MESD, editors. Primer to the Immune Response (Second Edition), Boston: Academic Cell; 2014, p. 181-196.

33. Chapter 4 - The B Cell Receptor: Proteins and Genes. In: Mak TW, Jett MESD, editors. Primer to the Immune Response (Second Edition), Boston: Academic Cell; 2014, p. 85-110.

34. Chapter 5 - B Cell Development, Activation and Effector Functions. In: Mak TW, Jett MESD, editors. Primer to the Immune Response (Second Edition), Boston: Academic Cell; 2014, p. 111-142.

35. JM Coffin. Hiv Population-Dynamics In-Vivo - Implications for Genetic-Variation, Pathogenesis, and Therapy. Science 1995;267:483-9.

36. DD Ho, AU Neumann, AS Perelson, W Chen, JM Leonard, M Markowitz. Rapid Turnover of Plasma Virions and Cd4 Lymphocytes in Hiv-1 Infection. Nature 1995;373:123-6.

37. XP Wei, SK Ghosh, ME Taylor, VA Johnson, EA Emini, P Deutsch, JD Lifson, S Bonhoeffer, MA Nowak, BH Hahn, SS Michael, MS George. Viral Dynamics in Human-Immunodeficiency-Virus Type-1 Infection. Nature 1995;373:117-22.

38. AS Perelson, AU Neumann, M Markowitz, JM Leonard, DD Ho. HIV-1 dynamics in vivo: Virion clearance rate, infected cell life-span, and viral generation time. Science 1996;271:1582-6.

39. MA Stafford, L Corey, YZ Cao, ES Daar, DD Ho, AS Perelson. Modeling plasma virus concentration during primary HIV infection. J Theor Biol 2000;203:285-301.

40. H Mohri, AS Perelson, K Tung, RM Ribeiro, B Ramratnam, M Markowitz, R Kost, A Hurley, L Weinberger, D Cesar, MK Hellerstein, DD Ho. Increased turnover of T lymphocytes in HIV-1 infection and its reduction by antiretroviral therapy. J Exp Med 2001;194:1277-87.

41. AS Perelson. Modelling viral and immune system dynamics. Nature Reviews Immunology 2002;2:28-36.

42. TJ Layden, JE Layden, RM Ribeiro, AS Perelson. Mathematical modeling of viral kinetics: a tool to understand and optimize therapy. Clin Liver Dis 2003;7:163-78.

43. ZD Ward, KAJ White, GAK van Voorn. Exploring the impact of target cell heterogeneity on HIV loads in a within-host model. Epidemics 2009;1:168-74.

44. AS Perelson, RM Ribeiro. Modeling the within-host dynamics of HIV infection. Bmc Biology 2013;11:96.

45. JE Layden-Almer, SJ Cotler, TJ Layden. Viral kinetics in the treatment of chronic hepatitis C. J Viral Hepat 2006;13:499-504.

46. RM Ribeiro, G Germanidis, KA Powers, B Pellegrin, P Nikolaidis, AS Perelson, JM Pawlotsky. Hepatitis B Virus Kinetics under Antiviral Therapy Sheds Light on Differences in Hepatitis B e Antigen Positive and Negative Infections. J Infect Dis 2010;202:1309-18.

47. A Busca, A Kumar. Innate immune responses in hepatitis B virus (HBV) infection. Virology Journal 2014;11:22.

48. JM Heffernan, MJ Keeling. An in-host model of acute infection: Measles as a case study. Theor Popul Biol 2008;73:134-47.

49. EW Larson, JW Dominik, AH Rowberg, GA Higbee. Influenza-Virus Population-Dynamics in Respiratory-Tract of Experimentally Infected Mice. Infect Immun 1976;13:438-47.

50. GA Bocharov, AA Romanyukha. Mathematical-Model of Antiviral Immune-Response-Iii - Influenza-a Virus-Infection. J Theor Biol 1994;167:323-60.

51. P Baccam, C Beauchemin, CA Macken, FG Hayden, AS Perelson. Kinetics of influenza A virus infection in humans. J Virol 2006;80:7590-9.

52. A Handel, IM Longini Jr., R Antia. Neuraminidase inhibitor resistance in influenza: Assessing the danger of its generation and spread. Plos Computational Biology 2007;3:2456-64.

53. HM Dobrovolny, R Gieschke, BE Davies, NL Jumbe, CAA Beauchemin. Neuraminidase inhibitors for treatment of human and avian strain influenza: A comparative modeling study. J Theor Biol 2011;269:234-44.

54. B Hancioglu, D Swigon, G Clermont. A dynamical model of human immune response to influenza A virus infection. J Theor Biol 2007;246:70-86.

55. A Handel, IM Longini Jr., R Antia. Towards a quantitative understanding of the within-host dynamics of influenza A infections. Journal of the Royal Society Interface 2010;7:35-47.

56. AM Smith, FR Adler, RM Ribeiro, RN Gutenkunst, JL McAuley, JA McCullers, AS Perelson. Kinetics of Coinfection with Influenza A Virus and Streptococcus pneumoniae. Plos Pathogens 2013;9:e1003238.

57. S Shrestha, B Foxman, S Dawid, AE Aiello, BM Davis, J Berus, P Rohani. Time and dose-dependent risk of pneumococcal pneumonia following influenza: a model for within-host interaction between influenza and Streptococcus pneumoniae. Journal of the Royal Society Interface 2013;10:20130233.

58. H Manchanda, N Seidel, A Krumbholz, A Sauerbrei, M Schmidtke, R Guthke. Within-host influenza dynamics: A small-scale mathematical modeling approach. BioSystems 2014;118:51-9.

59. KA Pawelek, D Dor Jr., C Salmeron, A Handel. Within-Host Models of High and Low Pathogenic Influenza Virus Infections: The Role of Macrophages. Plos One 2016;11:e0150568.

60. FA Ennis, A Meager, AS Beare, YH Qi, D Riley, G Schwarz, AH Rook. Interferon Induction and Increased Natural Killer-Cell Activity in Influenza Infections in Man. Lancet 1981;2:891-3.

61. CA Biron, KB Nguyen, GC Pien, LP Cousens, TP Salazar-Mather. Natural killer cells in antiviral defense: Function and regulation by innate cytokines. Annu Rev Immunol 1999;17:189-220.

62. X He, TH Holmes, C Zhang, K Mahmood, GW Kemble, DB Lewis, CL Dekker, HB Greenberg, AM Arvin. Cellular immune responses in children and adults receiving inactivated or live attenuated influenza vaccines. J Virol 2006;80:11756-66.

63. FJ Culley. Natural killer cells in infection and inflammation of the lung. Immunology 2009;128:151-63.

64. S Jost, H Quillay, J Reardon, E Peterson, RP Simmons, BA Parry, NN Bryant, WD Binder, M Altfeld. Changes in Cytokine Levels and NK Cell Activation Associated with Influenza. Plos One 2011;6:e25060.

65. GJ Bancroft. The Role of Natural-Killer-Cells in Innate Resistance to Infection. Curr Opin Immunol 1993;5:503-10.

66. GN Barber. Host defense, viruses and apoptosis. Cell Death Differ 2001;8:113-26.

67. WM Yokoyama. The role of natural killer cells in innate immunity to infection. Innate Immunity-Book 2003:321-39.

68. WM Yokoyama, SJ Kim, AR French. The dynamic life of natural killer cells. Annu Rev Immunol 2004;22:405-29.

69. Y Zhang, DL Wallace, CM de Lara, H Ghattas, B Asquith, A Worth, GE Griffin, GP Taylor, DF Tough, PCL Beverley, DC Macallan. In vivo kinetics of human natural killer cells: the effects of ageing and acute and chronic viral infection. Immunology 2007;121:258-65.

70. VJ Lisnic, A Krmpotic, S Jonjic. Modulation of natural killer cell activity by viruses. Curr Opin Microbiol 2010;13:530-9.

71. H Guo, P Kumar, S Malarkannan. Evasion of natural killer cells by influenza virus. J Leukoc Biol 2011;89:189-94.

72. H Mao, W Tu, Y Liu, G Qin, J Zheng, PL Chan, KT Lam, JS Peiris, YL Lau. Inhibition of Human Natural Killer Cell Activity by Influenza Virions and Hemagglutinin. J Virol 2010;84:4148-57.

73. A Fox, LNM Hoa, P Horby, HR van Doorn, NV Trung, NH Ha,NT Cap, VD Phu, NM Ha, DNT Ngoc, DVT Ngoc, HTT Kieu, WR Taylor, J farrar, H Wertheim, NV Kinh. Severe Pandemic H1N1 2009 Infection Is Associated with Transient NK and T Deficiency and Aberrant CD8 Responses. Plos One 2012;7:e31535.

74. L Canini, F Carrat. Population Modeling of Influenza A/H1N1 Virus Kinetics and Symptom Dynamics. J Virol 2011;85:2764-70.

75. SC Chen, SH You, CY Liu, CP Chio, CM Liao. Using experimental human influenza infections to validate a viral dynamic model and the implications for prediction. Epidemiol Infect 2012;140:1557-68.

76. DB Chang, CS Young. Simple scaling laws for influenza A rise time, duration, and severity. J Theor Biol 2007;246:621-35.

77. JJ Sedmak, SE Grossberg. Interferon Bioassay - Reduction in Yield of Myxovirus Neuraminidases. J Gen Virol 1973;21:1-7.

78. R Ben-Shachar, K Koelle. Minimal within-host dengue models highlight the specific roles of the immune response in primary and secondary dengue infections. Journal of the Royal Society Interface 2015;12:UNSP 20140886.

79. JJ Treanor, RF Betts, SM Erb, FK Roth, R Dolin. Intranasally Administered Interferon as Prophylaxis Against Experimentally Induced Influenza-a Virus-Infection in Humans. J Infect Dis 1987;156:379-83.

80. FG Hayden, AR Tunkel, JJ Treanor, RF Betts, S Allerheiligen, J Harris. Oral Ly217896 for Prevention of Experimental Influenza-a Virus-Infection and Illness in Humans. Antimicrob Agents Chemother 1994;38:1178-81.

81. FG Hayden, RS Fritz, MC Lobo, WG Alvord, W Strober, SE Straus. Local and systemic cytokine responses during experimental human influenza A virus infection - Relation to symptom formation and host defense. J Clin Invest 1998;101:643-9.

82. DP Calfee, AW Peng, LM Cass, M Lobo, FG Hayden. Safety and efficacy of intravenous zanamivir in preventing experimental human influenza A virus infection. Antimicrob Agents Chemother 1999;43:1616-20.

83. FG Hayden, JJ Treanor, RS Fritz, M Lobo, RF Betts, M Miller, N Kinnersley, P Ward, SE Straus. Use of the oral neuraminidase inhibitor oseltamivir in experimental human influenza - Randomized controlled trials for prevention and treatment. Jama-Journal of the American Medical Association 1999;282:1240-6.

84. L Kaiser, MS Briones, FG Hayden. Performance of virus isolation and Directigen (R) Flu A to detect influenza A virus in experimental human infection. Journal of Clinical Virology 1999;14:191-7.

85. RS Fritz, FG Hayden, DP Calfee, LMR Cass, AW Peng, WG Alvord, W Strober, SE Straus. Nasal cytokine and chemokine responses in experimental influenza A virus infection: Results of a placebo-controlled trial of intravenous zanamivir treatment. J Infect Dis 1999;180:586-93.

86. SI Tamura, T Kurata. Defense mechanisms against influenza virus infection in the respiratory tract mucosa. Jpn J Infect Dis 2004;57:236-47.

87. C Qiu, D Tian, Y Wan, W Zhang, C Qiu, Z Zhu, R Ye, Z Song, M Zhou, S Yuan, B Shi, M Wu, Y Liu, S Gu, J Wei, Z Zhou, X Zhang, Z Zhang, Y Hu, Z Yuan, J Xu. Early Adaptive Humoral Immune Responses and Virus Clearance in Humans Recently Infected with Pandemic 2009 H1N1 Influenza Virus. Plos One 2011;6:e22603.

88. N Baumgarth, OC Herman, GC Jager, L Brown, LA Herzenberg, LA Herzenberg. Innate and acquired humoral immunities to influenza virus are mediated by distinct arms of the immune system. Proc Natl Acad Sci U S A 1999;96:2250-5.

89. TP Hickling, X Chen, P Vicini, S Nayak. A review of quantitative modeling of B cell responses to antigenic challenge. Journal of Pharmacokinetics and Pharmacodynamics 2014;41:445-59.

APPENDIX

Please find below the e-mail stating that Figure 2 can be used in this thesis.

CDC INFO <cdcinfo@cdc.gov> Wed, Jun 29, 2016 at 12:31 PM

To: "akshsru12@gmail.com“ <akshsru12@gmail.com>

Thank you for your inquiry to CDC-INFO. We hope you find the following information about reproducing a figure from the CDC Weekly U.S. Influenza Surveillance Report website helpful.

You may use the figure in your thesis.

General text information, publications available for download, and graphs developed by CDC and found on the CDC website are works of the U.S. government and are in the public domain. These materials are meant for public use and a r e not subject to copyright laws. Permission is not required for use of public domain items. But, CDC does ask that you credit the original institution and contributor, when known, whenever the item is used in publicly distributed media.

You are also free to adapt and revise these materials, provided the information is distributed free of cost; however, you must remove the CDC name and logo if changes are made. Additionally, in accordance with 42 U.S.C. Section 1320b- 10, no person may, for a fee, reproduce, reprint, or distribute any item consisting of a form, application, or other publication of the U.S. Department of Health and Human Services (HHS) unless such person has obtained specific, written authorization to do so. Therefore, if you wish to sell CDC materials presented on the CDC website, you must first obtain permission from CDC.

Contact CDC
www.cdc.gov/contact/index3.htm

Thank you for contacting CDC-INFO. For more information, please call 1-800-CDC-INFO (800-232-4636), visit www.cdc.gov and click on “Contact CDC-INFO,” or go to www.cdc.gov/info. This e-mail is being sent from an unmonitored mailbox and CDC-INFO will not respond. If you have questions or comments, please send them via our online form at www.cdc.gov/info.

CDC-INFO is a service of the Centers for Disease Control and Prevention (CDC) and the Agency for Toxic Substances and Disease Registry (ATSDR). This service is provided by Verizon and its subcontractors under the Networks Universal contract to CDC and ATSDR.

----------Original Message ----------

From:
[cdcinfoforms@cdc.gov]
Sent: 6/28/2016 11:02 AM
To: cdcinfo@cdc.gov
Subject: CDCINFO:
Inquiry
Subject: Reproducing figure from CDC website
From: General Public
Email Address: akshsru12@gmail.com
Your Question:
Dear Team,

I am a graduate student at University of Illinois at Chicago (UIC) and I would like to use one of the figures given in the following link on CDC website in my thesis.

Link: http://www.cdc.gov/flu/weekly/
Title of figure: 122 Cities Mortality Reporting System

I will be including the above link in my citation and I will state in my text that source of the figure is from CDC web page. Please let me know if I require any other permission to use this figure other than citing the webpage in my thesis. Waiting for your reply.

Thanks & Regards,
Akshaya Polaepalli
Graduate student, dept. of chemical engineering
University of Illinois at Chicago (UIC)
Chicago, IL-60607

VITA

NAME:	Akshaya Sruthi Tirupathi Polaepalli
EDUCATION:	M.S., Chemical Engineering, University of Illinois at Chicago (UIC), Chicago, IL, 2016
	B.Tech., Chemical Engineering, St. Joseph's College of Engineering, Affiliated to Anna University, Chennai, Tamil Nadu, India, 2012
ACADEMIC EXPERIENCE:	Teaching Assistant (Jan 2016-May 2016) ChE382-Unit Operations Laboratory Supervisor: Dr. Alan Zdunek Department of Chemical Engineering, UIC
	Graduate Research Assistant (Jan 2015-July 2015) Advisor: Dr. Belinda Akpa Department of Chemical Engineering, UIC
	Undergraduate Research Assistant (Jan 2011-July 2013) Advisor: Dr. Tanmay Basak Department of Chemical Engineering Indian Institute of Technology Madras (IITM), India
INDUSTRIAL EXPERIENCE:	Senior System Executive (Sept 2012-July 2014) Cognizant Technology Solutions (CTS), Chennai, TN, India
	Summer Intern (May 2010-June 2010) Hindustan Coca-Cola Beverages Private Limited, India

PUBLICATIONS:

T.Basak, R.Anandalakshmi, T.P.A. Sruthi, “Analysis of Entropy Generation Due to Natural Convection for Hot and Cold Materials Confined within Two Entrapped Triangular Cavities”, Ind. Eng. Chem. Res. 2013, 52, 16414−16426.

T.Basak, A.K.Singh, T.P.A. Sruthi, S.Roy, “Finite element simulations on heat flow visualization and entropy generation during natural convection in inclined square cavities”, Int. Commun. Heat Mass Transf. 2014, 51, 1-8.

HONORS & AWARDS:

Customer Appreciation Award (Dec 2013, Apr 2014 & May 2014)
Cognizant Technology Solutions (CTS), Chennai, TN, India

Monthly Best Performance Award (May 2014)
Cognizant Technology Solutions (CTS), Chennai, TN, India

Special Award (May 2014)
Cognizant Technology Solutions (CTS), Chennai, TN, India

Best Newcomer Award (Jan 2013 & Apr 2013)
Cognizant Technology Solutions (CTS), Chennai, TN, India

Best Outgoing Student (2008-2012)
Department of Chemical Engineering, St. Joseph’s College of Engineering, Chennai, Tamil Nadu, India, 2012

Merit Scholarship, J.P.R. Educational Trust, St. Joseph’s College of Engineering, Chennai, Tamil Nadu, India, 2009